

**CARBON REMOVAL AND ELECTRICITY GENERATION USING TWO-
COMPARTMENT MICROBIAL FUEL CELL**

**M.Sc. Thesis by
Berfin Hatice ATAMERT**

Department : Environmental Engineering

Programme : Environmental Biotechnology

JANUARY 2011

CARBON REMOVAL AND ELECTRICITY GENERATION USING TWO-COMPARTMENT MICROBIAL FUEL CELL

**M.Sc. Thesis by
Berfin Hatice ATAMERT
(501081801)**

**Date of submission : 20 December 2010
Date of defence examination: 28 January 2011**

**Supervisor (Chairman) : Assoc. Prof. Dr. Ozlem KARAHAN (ITU)
Members of the Examining Committee : Prof. Dr. Nazik ARTAN (ITU)
Assoc. Prof. Dr. Didem AKCA GUVEN (FU)**

JANUARY 2011

İSTANBUL TEKNİK ÜNİVERSİTESİ ★ FEN BİLİMLERİ ENSTİTÜSÜ

**İKİ-BÖLMELİ MİKROBİYAL YAKIT HÜCRESİ KULLANARAK KARBON
GİDERİMİ VE ELEKTRİK ÜRETİMİ**

**YÜKSEK LİSANS TEZİ
Berfin Hatice ATAMERT
(501081801)**

Tezin Enstitüye Verildiği Tarih : 20 Aralık 2010

Tezin Savunulduğu Tarih : 28 Ocak 2011

**Tez Danışmanı : Doç. Dr. Özlem KARAHAN (İTÜ)
Diğer Jüri Üyeleri : Prof. Dr. Nazik ARTAN (İTÜ)
Doç. Dr. Didem AKÇA GÜVEN (FÜ)**

OCAK 2011

FOREWORD

First, I would like to thank Assoc. Prof. Dr. Ozlem KARAHAN for being my supervisor. I am very grateful for her guidance, encouragement, and understanding and for supporting this work. I will always be indebted to her for having me in her research group and giving me the chance to have a life-time experience of academic environment along with friends and colleagues.

I would also like to kindly thank Selcuk OZYURT , the head of Information Security and Special Systems Group (ISSS), Bahcesehir University, for his contribution to Set-up Studies and supervision of young researchers. My thanks go to all members of Information Security and Special Systems Group.

This study was supported by BAP Project No: 33613, “Asetat kullanan iki bölmeli mikrobiyal yakıt hücrelerinde karbon giderimi ve elektrik üretimi”.

On a personal note, I want to say thank you to my parents Tamer and Aysel ATAMERT, for their patience, love, believe in me, understanding and guide me to independence.

I thank all my other friends, especially Ozlem ARSLAN, who has been incredibly tolerant, helpful and friendly with me, for helping throughout my experimental studies.

Ocak 2011

Berfin Hatice ATAMERT
Environmental Engineer

TABLE OF CONTENTS

	<u>Page</u>
FOREWORD	v
TABLE OF CONTENTS	vii
ABBREVIATIONS	xi
LIST OF TABLES	xiii
LIST OF FIGURES	xv
SUMMARY	xix
ÖZET	xxi
1. INTRODUCTION	1
1.1 Meaning and Significance of the Thesis	1
1.2 Purpose and Scope of the Thesis.....	2
2. LITERATURE SURVEY	3
2.1 Process of Microbial Fuel Cell.....	3
2.2 Components of Microbial Fuel Cell.....	5
2.3 History of Microbial Fuel Cell Development	6
2.4 Applications of Microbial Fuel Cell	8
2.4.1 Electricity generation	8
2.4.2 Biohydrogen.....	9
2.4.3 Wastewater treatment.....	9
2.4.4 Biosensor.....	10
2.5 Design of Microbial Fuel Cell	11
2.5.1 Two-compartment MFC systems.....	11
2.5.2 Single-compartment MFC systems	13
2.5.3 Up-flow mode MFC systems	15
2.5.4 Stacked microbial fuel cell.....	16
2.6 Performance of Microbial Fuel Cell	17
2.6.1 Ideal performance of MFC.....	17
2.6.2 Actual performance of MFC	18
2.7 Effects of Operation Conditions.....	19
2.7.1 Effect of electrode materials	19
2.7.2 pH buffer and electrolyte	21
2.7.3 Proton exchange system.....	21
2.7.4 Operating conditions in the anodic chamber.....	22
2.7.5 Operating conditions in the cathodic chamber.....	23
3. MATERIALS AND METHODS	25

3.1 The Preliminary Work for the Setup of the MFC System.....	25
3.1.1 Acclimation period	25
3.1.2 Start-up period of MFC	26
3.1.2.1 MFC design	26
3.1.2.2 Set-up and start-up operation of the system	28
3.2 Analysis Conducted and Calculated Parameters in the MFC System.....	29
4. EXPERIMENTAL RESULTS	33
4.1 The Preliminary Experimental Results	33
4.1.1 Acclimation period	33
4.1.1.1 COD profiles	33
4.1.1.2 MLSS-MLVSS profile	34
4.1.2 Start-up period results	35
4.1.2.1 COD profiles	35
4.1.2.2 MLSS-MLVSS profiles.....	36
4.1.2.3 Electricity generation profile.....	36
4.2 MFC Experiment Results for Different COD Concentrations	37
4.2.1 MFC results for 325 mg/l COD concentration without external resistance.....	37
4.2.1.1 COD profiles	37
4.2.1.1.1 COD profiles without suspended biomass	37
4.2.1.1.2 COD profiles with suspended biomass	38
4.2.1.2 MLSS and MLVSS profiles	39
4.2.1.3 pH profile.....	39
4.2.1.4 Voltage profiles	40
4.2.1.4.1 Voltage profile without suspended biomass.....	40
4.2.1.4.2 Voltage profile with suspended biomass.....	41
4.2.1.5 COD and OCV profile.....	41
4.2.2 MFC results for 325 mg/l COD concentration with external resistance.....	42
4.2.2.1 COD profiles	42
4.2.2.2 MLSS and MLVSS profiles	43
4.2.2.3 pH profile.....	44
4.2.2.4 Voltage profile with suspended biomass and 1 k Ω resistance	44
4.2.2.5 Power and current profile	45
4.2.2.6 Density profiles	45
4.2.2.7 Polarization curve experiment for 325 mg/l COD	46
4.2.3 MFC results for 650 mg/l COD concentration without external resistance.....	46
4.2.3.1 Voltage and COD profile	46
4.2.4 MFC results for 650 mg/l COD concentration with external resistance... ..	47
4.2.4.1 COD profiles	47
4.2.4.2 MLSS and MLVSS profiles	48
4.2.4.3 pH profile	49
4.2.4.4 Voltage profile with suspended biomass and 1 k Ω resistance	49
4.2.4.5 Power and current profile	50
4.2.4.6 Density profiles	50
4.2.4.7 Polarization curve experiment result for 650 mg/l COD	51

4.2.5 MFC results for 160 mg/l COD concentration without external resistance.....	51
4.2.5.1 Voltage and COD profile	51
4.2.6 MFC results for 160 mg/l COD concentration with external resistance....	52
4.2.6.1 COD profiles	52
4.2.6.2 MLSS and MLVSS profiles	53
4.2.6.3 pH profile.....	53
4.2.6.4 Voltage profile with suspended biomass and 1 k Ω resistance	54
4.2.6.5 Power and current profile.....	54
4.2.6.6 Density profiles	55
4.2.6.7 Polarization curve experiment result for 160 mg/l.....	55
5. RESULT AND DISCUSSION.....	57
REFERENCES.....	65
CIRRICULUM VITAE.....	71

ABBREVIATIONS

BOD	: Biological Oxygen Demand
CE	: Coulombic efficiency
COD	: Chemical Oxygen Demand
DO	: Dissolved Oxygen
FPMFC	: Flat Plate Microbial Fuel Cell
I	: Current
I_{AN}	: Anodic Current Density
MFC	: Microbial Fuel Cell
MLSS	: Suspended Solid
MLVSS	: Volatile Suspended Solid
OCV	: Open Circuit Voltage
P	: Power
P_{AN}	: Anodic Power Density
PEM	: Proton Exchange Membrane
Pt	: Platinum
SCMFC	: Single Compartment Microbial Fuel Cell
TEA	: Terminal Electron Acceptor
V	: Voltage

LIST OF TABLES

	<u>Page</u>
Table 2.1: Basic components of microbial fuel cells (Du et. al., 2007).....	5
Table 3.1: Summary of the operation conditions and the parameters were investigated during the experiments	32
Table 5.1: Overview of the experimental results for the MFC system under different feeding conditions.....	62

LIST OF FIGURES

	<u>Page</u>
Figure 2.1 : Schematic diagram of a typical two-chamber microbial fuel cell (Du et al., 2007).....	4
Figure 2.2 : Schematics of a two-compartment MFC in cylindrical shape (A), rectangular shape (B), miniature shape (C), upflow configuration with cylindrical shape (D), cylindrical shape with an U-shaped cathodic compartment (E). (Fig. 4A drawn to illustrate a photo in Min et al., 2005a,b. The rest drawn with modifications after Delaney et al., 1984; Allen and Bennetto, 1993; Ringeisen et al., 2006; He et al., 2005, 2006, respectively.)	12
Figure 2.3 : Schematics of side views of a flat plate MFC. (Figures drawn with modifications after Min and Logan, 2004.).....	13
Figure 2.4 : An MFC with a proton permeable layer coating the inside of the window-mounted cathode (A), an MFC consisting of an anode and cathode placed on opposite side in a plastic cylindrical chamber (B), and a tubular MFC with outer cathode and inner anode consisting of graphite granules (C). ((A) drawn to illustrate a photo in Park and Zeikus, 2003. (B) and (C) drawn with modifications after Liu and Logan, 2004; Rabaey et al., 2005b, respectively.)	14
Figure 2.5 : Schematics of a cylindrical SCMFC containing eight graphite rods as an anode in a concentric arrangement surrounding a single cathode. ((A) drawn with modifications after Liu et al., 2004. (B) drawn to illustrate a photo in Liu et al., 2004.)	15
Figure 2.6 : Schematics of mediator-and membrane-less MFC with cylindrical shape (A), and with rectangular shape (B). (Figures drawn with modifications after Jang et al., 2004; Tartakovsky and Guiot, 2006, respectively.)....	16
Figure 2.7 : Stacked MFCs consisting of six individual units with granular graphite anode. (Figure drawn to illustrate a photo in Aelterman et al., 2006.) .	17
Figure 3.1 : The acclimation reactor	25
Figure 3.2 : Materials which are necessary for the start-up period of the microbial fuel.....	27
Figure 3.3 : Experimental set up of microbial fuel cell	28
Figure 4.1 :Influent and effluent COD concentration in the acclimation reactor.....	33
Figure 4.2 :COD removal efficiency in the acclimation reactor.....	34
Figure 4.3 :MLSS-MLVSS concentrations in the acclimation reactor.....	34
Figure 4.4 :Influent and effluent COD concentration in the start-up MFC reactor.....	35

Figure 4.5: COD removal efficiency in the start-up MFC reactor	35
Figure 4.6: MLSS-MLVSS concentrations in the start-up MFC reactor	36
Figure 4.7: Electricity generation in the start-up MFC reactor	36
Figure 4.8: Influent and effluent COD concentrations and COD removal efficiencies of the MFC reactor without suspended biomass	37
Figure 4.9: COD removal of the MFC reactor without suspended biomass	38
Figure 4.10: Influent and effluent COD concentrations and COD removal efficiencies of the MFC reactor with suspended biomass	38
Figure 4.11: COD removal of the MFC reactor with suspended biomass	39
Figure 4.12: MLSS-MLVSS concentrations in the MFC reactor	39
Figure 4.13: pH profiles of the MFC reactor with suspended biomass	40
Figure 4.14: Voltage profile without suspended biomass	40
Figure 4.15: Voltage profile with suspended biomass	41
Figure 4.16: COD and OCV profile in the MFC fed with 325 mg/l COD without resistance.....	42
Figure 4.17: Influent and effluent COD concentrations and COD removal efficiencies in the MFC reactor fed with 325 mg/l COD	42
Figure 4.18: COD removal in the MFC reactor fed with 325 mg/l COD	43
Figure 4.19: MLSS-MLVSS concentrations in the MFC reactor fed with 325 mg/l COD.....	43
Figure 4.20: pH profiles in the MFC reactor fed with 325 mg/l COD.....	44
Figure 4.21: Voltage profile in the MFC fed with 325 mg/l COD	44
Figure 4.22: Current and power profiles in MFC fed with 325 mg/l COD	45
Figure 4.23: Current and power density profiles in MFC fed with 325 mg/l COD.....	45
Figure 4.24: Polarization curve in the MFC fed with 325 mg/l COD.....	46
Figure 4.25: COD and OCV profile in the MFC fed with 650 mg/l COD without resistance.....	47
Figure 4.26: Influent and effluent COD concentrations and COD removal efficiencies in the MFC reactor fed with 650 mg/l COD	47
Figure 4.27: COD removal in the MFC reactor fed with 650 mg/l COD	48
Figure 4.28: MLSS-MLVSS concentrations in the MFC reactor fed with 650 mg/l COD	48
Figure 4.29: pH profiles in the MFC reactor fed with 650 mg/l COD.....	49
Figure 4.30: Voltage profile in the MFC fed with 650 mg/l COD	49
Figure 4.31: Current and power profiles in MFC fed with 650 mg/l COD.....	50
Figure 4.32: Current and power density profiles in MFC fed with 650 mg/l COD.....	50
Figure 4.33: Polarization curve in the MFC fed with 650 mg/l COD.....	51
Figure 4.34: COD and OCV profile in the MFC fed with 160 mg/l COD without resistance.....	51
Figure 4.35: Influent and effluent COD concentrations and COD removal efficiencies in the MFC reactor fed with 160 mg/l COD	52
Figure 4.36: COD removal in the MFC reactor fed with 160 mg/l COD	52
Figure 4.37: MLSS-MLVSS concentrations in the MFC reactor fed with 160 mg/l COD.....	53
Figure 4.38: pH profiles in the MFC reactor fed with 650 mg/l COD.....	53
Figure 4.39: Voltage profile in the MFC fed with 160 mg/l COD	54

Figure 4.40: Current and power profiles in MFC fed with 160 mg/l COD	54
Figure 4.41: Current and power density profiles in MFC fed with 160 mg/l COD.....	55
Figure 4.42: Polarization curve in the MFC fed with 160 mg/l COD	55
Figure 5.1: OCV profile for each substrate concentration.....	57
Figure 5.2: Maximum voltage profiles for each substrate concentration.....	57
Figure 5.3: Maximum power density profile for each substrate concentration.....	58
Figure 5.4: Maximum current density profile for each substrate concentration.....	58
Figure 5.5: Polarization curves of MFC system for different COD concentrations.....	59
Figure 5.6: Internal resistance of MFC system for different COD concentrations.....	60
Figure 5.7: COD removal efficiency profile for each substrate concentration.....	60
Figure 5.8: CE profile for each substrate concentration.....	61

CARBON REMOVAL AND ELECTRICITY GENERATION USING TWO-COMPARTMENT MICROBIAL FUEL CELL

SUMMARY

In recent years, research activity on microbial fuel cell (MFC) technology has increased markedly. This technology consists of electrochemical reactors which generate electricity directly from an organic fuel using micro-organisms. Electricity generation from a MFC using fermentation products and waste organics as fuel has been well documented. However, the greatest potential for practical application of MFCs is in wastewater treatment. In fact, this is a prospectively important subject not for present applications but for future ones. Nowadays, the costs associated with the treatment of wastewaters are very high and the development of a technology that allows to simultaneously treat a waste and to directly produce energy would have a very high significance.

Unfortunately, the efficiencies obtained presently in MFCs are far away from those required for commercial applications, and a lot of fundamental work has to be done in order to develop a ready-to-use technology.

In this work, the production of electricity and the oxidation of the pollutants contained in a synthetic wastewater fed with sodium acetate as carbon source, using a mediator-less two-compartment microbial fuel cell was studied. To this end, this thesis consisted of three stages.

At the beginning the activated sludge which was taken from Bahçeşehir Domestic Wastewater Treatment Plant has been acclimated for 3 months.

Secondly, MFC set-up phase was carried out.

Last phase was experiments in MFC. During the MFC experiment phase, it was observed that with high hydraulic and solid retention times it is possible to obtain a very efficient process with respect to Chemical Oxygen Demand (COD) removal and electricity generation. The volatile suspended solid (MLVSS) concentration of the studied activated sludge was 1500 mg/l. Moreover, the effect of feeding synthetic wastewater with the same composition, but with the different COD concentrations, was studied.

The parameters such as COD, MLVSS, pH, voltage (V), current (I), power (P), anodic power density (P_{AN}), anodic current density (I_{AN}) was investigated under different feeding conditions.

İKİ-BÖLMELİ MİKROBİYAL YAKIT HÜCRESİ KULLANARAK KARBON GİDERİMİ VE ELEKTRİK ÜRETİMİ

ÖZET

Son yıllarda, mikrobiyal yakıt hücresi (MYH) teknolojisi hakkında yapılan araştırmalar belirgin bir şekilde artmıştır. Bu teknoloji, mikroorganizmalar tarafından kullanılan organik yakıtı doğrudan elektriğe çeviren elektrokimyasal reaktörlerden oluşmaktadır. Fermentasyon ürünlerinin ve organik atıkların yakıt olarak kullanıldığı MYH'den elektrik üretimi pek çok çalışma ile belgelenmiştir. Ancak, MYH'nin pratik uygulamaları için en büyük olanak atıksu arıtmadır. Aslında, bu şimdiki uygulamalar için değil gelecektekiler için önemli bir konudur. Günümüzde, atık suların arıtımı ile ilişkili maliyetler çok yüksektir ve kendiliğinden bir atığın arıtılmasına ve doğrudan enerji üretilmesine olanak sağlayan bir teknolojinin geliştirilmesi çok yüksek bir öneme sahip olacaktır.

Ancak, bugüne kadar ki çalışmalarda elde edilen verimler, ticari uygulamalar için gerekli olanlardan çok uzaktır ve kullanıma hazır bir teknoloji geliştirmek için gelecek yıllar boyunca pek çok temel çalışma yapılmalıdır.

Bu çalışmada, mediatörsüz (aracısız) iki bölmeli mikrobiyal yakıt hücresi kullanılarak, elektrik üretimi ve karbon kaynağı olarak sodyum asetat ile beslenen sentetik atıksudaki organik kirleticinin oksidasyonu incelenmiştir. Bu amaçla, bu tez üç aşamadan oluşmaktadır.

Başlangıçta Bahçeşehir Eysel Atıksu Arıtma Tesisinden alınan aktif çamur 3 ay boyunca aklime edilmiştir.

İkinci olarak, MYH kurulum çalışması yürütülmüştür.

Son aşama, MYH ile yürütülen deneylerden oluşmaktadır. MFC deneyleri aşaması boyunca, yüksek hidrolik ve çamur bekletme sürelerinde elektrik üretimi ve Kimyasal Oksijen İhtiyacı (KOİ) giderimi ile çok verimli bir proses elde etmenin mümkün olduğu gözlemlenmiştir. Çalışmada kullanılan aktif çamur uçucu askıda katı madde (UAKM) konsantrasyonu 1500 mg/l'dir. Bundan başka, aynı bileşime sahip sentetik atıksuyun farklı KOİ konsantrasyonları ile çalışılmıştır.

KOİ, UAKM, pH, voltaj (V), akım (I), güç (P), güç yoğunluğu (P_{AN}), ve akım yoğunluğu (I_{AN}) gibi parametreler incelenmiştir.

1. INTRODUCTION

1.1 Meaning and Significance of the Thesis

A technology using microbial fuel cells that convert the energy stored in chemical bonds of organic compounds to electrical energy achieved through the catalytic reactions by microorganisms, has generated considerable interest among academic researchers in recent years (Allen and Bennetto, 1993; Gil et al., 2003; Moon et al., 2006; Choi et al., 2003).

In the past decade, rapid advances have been made in MFC research and the number of journal publications has increased sharply in the past three years with more researchers joining the research field. Several reviews on MFC are available, each with a different flavor or emphasis. Logan et al. (2006) reviewed MFC designs, characterizations and performances. The microbial metabolism in MFCs was reviewed by Rabaey and Verstraete (2005). Lovley (2006) mainly focused his review on the promising MFC systems known as Benthic Unattended Generators (BUGs) for powering remote-sensing or monitoring devices from the angle of microbial physiologies. Pham et al. (2006) summarized the advantages and disadvantages of MFCs compared to the conventional anaerobic digestion technology for the production of biogas as renewable energy. Chang et al. (2006) discussed both the properties of electrochemically active bacteria used in mediatorless MFC and the rate limiting steps in electron transport. Bullen et al. (2006) compiled many experimental results on MFCs reported recently in their review on biofuel cells.

The use of fossil fuels, especially oil and gas, in recent years has accelerated and this triggers a global energy crisis. Renewable bioenergy is viewed as one of the ways to alleviate the current global warming crisis. Major efforts are devoted to developing alternative electricity production methods. Electricity production from renewable resources without producing carbon dioxide emission is the key for global warming (Lovley, 2006, Davis and Higson, 2007).

1.2 Purpose and Scope of the Thesis

The aim of this thesis is to study the performance of an MFC fed with synthetic wastewater consisting of sodium acetate as the substrate. The work is focused on the study of acclimation of the microbial culture and on the effect of the concentration of the substrate, paying special attention to the study of the relationship between COD removal and electricity production, including the achievement of a high power and current density. For this reason, the hydraulic and solid retention times of the MFC were selected to be enough to assure the degradation of the organic substrate. A two-compartment MFC with the anodic and the cathodic chambers separated by a proton exchange membrane (PEM) was used. In this scope, carbon removal and electricity generation efficiencies were observed for different sodium acetate concentrations which were 325 mg COD/l, 650 mg COD/l, and 160 mg COD/l.

In the first chapter, the meaning and significance of the subject, the purpose and scope of the Thesis are presented.

In the second chapter, a review on MFC with emphases on the recent advances in MFC reactor designs, MFC performances, applications and optimization of important operating parameters and a brief MFC research history are presented.

In the third chapter, methods used in experimental studies, materials used in the applied analysis are given.

In the fourth chapter, experimental studies are presented. The data obtained from experimental studies are shown and interpreted.

In the fifth chapter, a general evaluation of the experimental studies is provided and the conclusions are presented.

2. LITERATURE SURVEY

2.1 Process of Microbial Fuel Cell

Microbial fuel cell technologies represent the newest approach for generating electricity-bioelectricity generation from biomass using bacteria. In an MFC, microorganisms degrade (oxidize) organic matter, producing electrons that travel through a series of respiratory enzymes in the cell and make energy for the cell in the form of ATP. The electrons are then released to a terminal electron acceptor (TEA) which accepts the electrons and becomes reduced. For example, oxygen can be reduced to water through a catalyzed reaction of the electrons with protons. Many TEAs such as oxygen, nitrate, sulfate, and others readily diffuse into the cell where they accept electrons forming products that can diffuse out of the cell. However, we now know that some bacteria can transfer electrons exogenously (*i.e.*, outside the cell) to a TEA such as a metal oxide like iron oxide. These bacteria that can exogenously transfer electrons, called *exoelectrogens*, can be used to produce power in an MFC. In line with the common nomenclature for categorizing biochemical process, microorganisms, and reactors are classified. Therefore, this method of electron-generating process is entitled as *electrogenesis*, with the bacteria called *exoelectrogens* and in the reactor named as a *microbial fuel cell*.

Bacteria can be used in MFCs to generate electricity while accomplishing the biodegradation of organic matters or wastes (Park and Zeikus, 2000; Oh and Logan., 2005). Fig. 2.1 shows a schematic diagram of a typical MFC for producing electricity. It consists of anodic and cathodic chambers separated by a proton exchange membrane (Wilkinson, 2000; Gil et al., 2003).

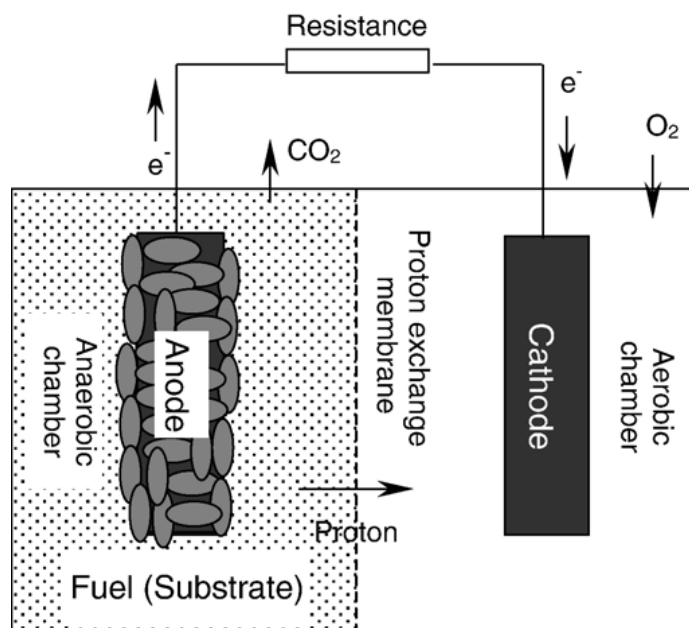


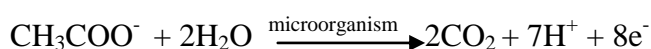
Figure 2.1 : Schematic diagram of a typical two-chamber microbial fuel cell (Du et al., 2007).

Microorganisms in the anodic chamber of an MFC oxidize added substrates and generate electrons and protons in the process. Carbon dioxide is produced as an oxidation product. However, there is no net carbon emission because the carbon dioxide in the renewable biomass originally comes from the atmosphere in the photosynthesis process. Unlike in a direct combustion process, the electrons are absorbed by the anode and are transported to the cathode through an external circuit. After crossing a PEM or a salt bridge, the protons enter the cathodic chamber where they combine with oxygen to form water. Microorganisms in the anodic chamber extract electrons and protons in the dissimilative process of oxidizing organic substrates (Rabaey and Verstraete, 2005).

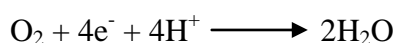
Electric current generation is possible by keeping microorganisms separated from oxygen or any other terminal acceptor other than the anode and this requires an anaerobic anodic chamber.

Typical electrode reactions are shown below using acetate as a model substrate.

Anodic reaction :



Cathodic reaction :



The overall reaction is the breakdown of the substrate to carbon dioxide and water with a concomitant production of electricity as a by-product. Based on the electrode reaction pair above, an MFC bioreactor can generate electricity from the electron flow from the anode to cathode in the external circuit.

2.2 Components of Microbial Fuel Cell

A typical MFC consists of an anodic chamber and a cathodic chamber separated by a proton exchange membrane as shown in Fig. 2.1. A one-compartment MFC eliminates the need for the cathodic chamber by exposing the cathode directly to the air. Table 2.1 shows a summary of MFC components and the materials used to construct them (Logan et al., 2006; Rabaey and Verstraete, 2005; Bullen et al., 2006; Lovley, 2006).

Table 2.1: Basic components of microbial fuel cells (Du et al., 2007).

Items	Materials	Remarks
Anode	Graphite, graphite felt, carbon paper-cloth, Pt, Pt black, reticulated vitreous carbon (RVC)	Necessary
Cathode	Graphite, graphite felt, carbon paper, carbon-cloth, Pt, Pt black, RVC	Necessary
Anodic Chamber	Glass, polycarbonate, Plexiglas	Necessary
Cathodic Chamber	Glass, polycarbonate, Plexiglas	Optional
Proton Exchange Membrane	Proton exchange membrane:Nafion, Ultrex, polyethylene.poly (styrene-codivinybenzene); salt bridge, porcelain septum or solely electrolyte	Necessary
Electrode catalyst	Pt, Pt black, MnO ₂ , Fe ³⁺ , polyaniline, electron mediator immobilized on anode	Optional

2.3 History of Microbial Fuel Cell Development

Theoretically, most microorganisms can potentially be used as a biocatalyst in MFC. The earliest MFC concept was demonstrated by Potter in 1910 (Ieropoulos, 2005a).

Electrical energy was produced from living cultures of *Escherichia coli* and *Saccharomyces* by using platinum (Pt) electrodes (Potter, 1912).

This did not generate much interest until 1980s when it was discovered that current density and the power output could be greatly enhanced by the addition of electron mediators. Unless the species in the anodic chamber are anodophiles, the microorganisms are incapable of transferring electrons directly to the anode. The outer layers of the majority of microbial species are composed of non-conductive lipid membrane, peptidoglycans and lipopolysaccharides that hinder the direct electron transfer to the anode. Electron mediators accelerate the transfer (Davis and Higson, 2007).

Mediators in an oxidized state can easily be reduced by capturing the electrons from within the membrane. The mediators then move across the membrane and release the electrons to the anode and become oxidized again in the bulk solution in the anodic chamber. This cyclic process accelerates the electron transfer rate and thus increases the power output. Good mediators should possess the following features (Ieropoulos et al., 2005a):

- (1) able to cross the cell membrane easily;
- (2) able to grab electrons from the electron carriers of the electron transport chains;
- (3) possessing a high electrode reaction rate;
- (4) having a good solubility in the anolyte;
- (5) nonbiodegradable and non-toxic to microbes;
- (6) low cost.

How efficient the oxidized mediator gets reduced by the cells reducing power is more important compared with other features. Although a mediator with the lowest redox would in theory give the lowest anodic redox and thus maximize the redox difference between anode and cathode (i.e. give biggest voltage difference) it would not necessarily be the most efficient at pulling electrons away from the reduced

intracellular systems within the microbes. A mediator with a higher E_0 redox would give a higher overall power than a mediator with the lowest redox (Ieropoulos et al., 2005a).

Typical synthetic exogenous mediators include dyes and metallorganics such as neutral red, methylene blue, thionine, meldola's blue, 2-hydroxy-1,4-naphthoquinone, and Fe(III)EDTA (Park and Zeikus, 2000; Tokuji and Kenji, 2003; Vega and Fernandez, 1987; Allen and Bennetto, 1993; Ieropoulos et al., 2005a).

Unfortunately, the toxicity and instability of synthetic mediators limit their applications in MFCs. Some microorganisms can use naturally occurring compounds including microbial metabolites (Endogenous mediators) as mediators. Humic acids, anthraquinone, the oxyanions of sulphur (sulphate and thiosulphate) all have the ability to transfer electrons from inside the cell membrane to the anode (Lovley, 1993).

A real breakthrough was made when some microorganisms were found to transfer electrons directly to the anode (Kim et al., 1999a, Chaudhuri and Lovley, 2003).

These microorganisms are operationally stable and yielded a high Coulombic Efficiency (CE) (Chaudhuri and Lovley, 2003; Scholz and Schroder, 2003). *Shewanella putrefaciens* (Kim et al., 2002), *Geobacteraceae sulfurreducens* (Bond and Lovley, 2003), *Geobacter metallireducens* (Min et al., 2005a) and *Rhodospirillum rubrum* (Chaudhuri and Lovley, 2003) are all bioelectrochemically active and can form a biofilm on the anode surface and transfer electrons directly by conductance through the membrane. When they are used, the anode acts as the final electron acceptor in the dissimilatory respiratory chain of the microorganisms in the biofilm. Biofilms forming on a cathode surface may also play an important role in electron transfer between the microbes and the electrodes. Cathodes can serve as electron donors for *Thiobacillus ferrooxidans* suspended in a catholyte (Prasad et al., 2006) for an MFC system that contained microorganisms in both anodic and cathodic chambers. *G. Metallireducens* and *G. sulfurreducens* (Gregory et al., 2004) or other seawater biofilms (Bergel et al., 2005) may all act as final electron acceptors by grabbing the electrons from cathode as electron donors. Since the cost of a mediator is eliminated, mediator-less MFCs are advantageous in wastewater treatment and power generation (Ieropoulos et al., 2005a).

2.4 Applications of Microbial Fuel Cell

2.4.1 Electricity generation

MFCs are capable of converting the chemical energy stored in the chemical compounds in a biomass to electrical energy with the aid of microorganisms. Because chemical energy from the oxidation of fuel molecules is converted directly into electricity instead of heat, the Carnot cycle with a limited thermal efficiency is avoided and theoretically a much higher conversion efficiency can be achieved (70%) just like conventional chemical fuel cells. Chaudhury and Lovley (2003) reported that *R. ferrireducens* could generate electricity with an electron yield as high as 80%. Higher electron recovery as electricity of up to 89% was also reported (Rabaey et al., 2003). An extremely high Coulombic Efficiency of 97% was reported during the oxidation of formate with the catalysis of Pt black (Rosenbaum et al., 2006). However, MFC power generation is still very low (Tender et al., 2002; Delong and Chandler, 2002), that is the rate of electron abstraction is very low. One feasible way to solve this problem is to store the electricity in rechargeable devices and then distribute the electricity to end-users (Ieropoulos et al., 2003a). Capacitors were used in their biologically inspired robots named EcoBot I to accumulate the energy generated by the MFCs and worked in a pulsed manner. MFCs are especially suitable for powering small telemetry systems and wireless sensors that have only low power requirements to transmit signals such as temperature to receivers in remote locations (Ieropoulos et al., 2005c; Shantaram et al., 2005). MFCs themselves can serve as distributed power systems for local uses, especially in underdeveloped regions of the world. MFCs are viewed by some researchers as a perfect energy supply candidate for Gastrobots by self-feeding the biomass collected by themselves (Wilkinson, 2000). Realistic energetically autonomous robots would probably be equipped with MFCs that utilize different fuels like sugar, fruit, dead insects, grass and weed. The robot EcoBot-II solely powers itself by MFCs to perform some behavior including motion, sensing, computing and communication (Ieropoulos et al., 2003b; Ieropoulos et al., 2004; Melhuish et al., 2006). Locally supplied biomass can be used to provide renewable power for local consumption. Applications of MFCs in a spaceship are also possible. The MFC technology is particularly favored for sustainable long-term power applications. However, only after potential health

and safety issues brought by the microorganisms in the MFC are thoroughly solved, could it be applied for this purpose.

2.4.2 Biohydrogen

MFCs can be readily modified to produce hydrogen instead of electricity. Under normal operating conditions, protons released by the anodic reaction migrate to the cathode to combine with oxygen to form water. Hydrogen generation from the protons and the electrons produced by the metabolism of microbes in an MFC is thermodynamically unfavorable. Liu et al. (2005c) applied an external potential to increase the cathode potential in a MFC circuit and thus overcame the thermodynamic barrier. In this mode, protons and electrons produced by the anodic reaction are combined at the cathode to form hydrogen. The required external potential for an MFC is theoretically 110 mV, much lower than the 1210 mV required for direct electrolysis of water at neutral pH because some energy comes from the biomass oxidation process in the anodic chamber. MFCs can potentially produce about 8–9 mol H₂/mol glucose compared to the typical 4 mol H₂/mol glucose achieved in conventional fermentation (Liu et al., 2005c). In biohydrogen production using MFCs, oxygen is no longer needed in the cathodic chamber. Thus, MFC efficiencies improve because oxygen leak to the anodic chamber is no longer an issue. Another advantage is that hydrogen can be accumulated and stored for later usage to overcome the inherent low power feature of the MFCs. Therefore, MFCs provide a renewable hydrogen source that can contribute to the overall hydrogen demand in a hydrogen economy (Holzman, 2005).

2.4.3 Wastewater treatment

The MFCs were considered to be used for treating waste water early in 1991 (Habermann and Pommer, 1991). Municipal wastewater contains a multitude of organic compounds that can fuel MFCs. The amount of power generated by MFCs in the wastewater treatment process can potentially halve the electricity needed in a conventional treatment process that consumes a lot of electric power aerating activated sludges. MFCs yield 50–90% less solids to be disposed of (Holzman, 2005). Furthermore, organic molecules such as acetate, propionate, and butyrate can be thoroughly broken down to CO₂ and H₂O. A hybrid incorporating both electrophiles and anodophiles are especially suitable for wastewater treatment

because more organics can be biodegraded by a variety of organics. MFCs using certain microbes have a special ability to remove sulfides as required in wastewater treatment (Rabaey et al., 2006). MFCs can enhance the growth of bioelectrochemically active microbes during wastewater treatment thus they have good operational stabilities. Continuous flow and single-compartment MFCs (SCMFC) and membrane-less MFCs are favored for wastewater treatment due to concerns in scale-up (Jang et al., 2004; Moon et al., 2005; He et al., 2005). Sanitary wastes, food processing wastewater, swine wastewater and corn stover are all great biomass sources for MFCs because they are rich in organic matters (Suzuki et al., 1978; Liu et al., 2004; Oh and Logan, 2005; Min et al., 2005b; Zuo et al., 2006). Up to 80% of the COD can be removed in some cases (Liu et al., 2004; Min et al., 2005b) and a Coulombic efficiency as high as 80% has been reported (Kim et al., 2005).

2.4.4 Biosensor

Apart from the aforementioned applications, another potential application of the MFC technology is to use it as a sensor for pollutant analysis and in situ process monitoring and control (Chang et al., 2004, 2005). The proportional correlation between the Coulombic yield of MFCs and the strength of the wastewater make MFCs possible biological oxygen demand (BOD) sensors (Kim et al., 2003). An accurate method to measure the BOD value of a liquid stream is to calculate its Coulombic yield. A number of works (Chang et al., 2004; Kim et al., 2003) showed a good linear relationship between the Coulombic yield and the strength of the wastewater in a quite wide BOD concentration range. However, a high BOD concentration requires a long response time because the Coulombic yield can be calculated only after the BOD has been depleted unless a dilution mechanism is in place. Efforts have been made to improve the dynamic responses in MFCs used as sensors (Moon et al., 2004). A low BOD sensor can also show the BOD value based on the maximum current since the current values increase with the BOD value linearly in an oligotroph-type MFC. During this stage, the anodic reaction is limited by substrate concentration. This monitoring mode can be applied to real-time BOD determinations for either surface water, secondary effluents or diluted high BOD wastewater samples (Kang et al., 2003). MFC-type of BOD sensors are advantageous over other types of BOD sensor because they have excellent operational stability and good reproducibility and accuracy. An MFC-type BOD sensor constructed with the

microbes enriched with MFC can be kept operational for over 5 years without extra maintenance (Kim et al., 2003), far longer in service life span than other types of BOD sensors reported in the literature.

2.5 Design of Microbial Fuel Cell

2.5.1 Two-compartment MFC systems

Two-compartment MFCs are typically run in batch mode often with a chemically defined medium such as glucose or acetate solution to generate energy. They are currently used only in laboratories. A typical two compartment MFC has an anodic chamber and a cathodic chamber connected by a PEM, or sometimes a salt bridge, to allow protons to move across to the cathode while blocking the diffusion of oxygen into the anode.

The compartments can take various practical shapes. The schematic diagrams of five two-compartment MFCs are shown in Fig. 2.2 The mini-MFC shown in Fig. 2.2 C having a diameter of about 2 cm, but with a high volume power density was reported by Ringeisen et al. (2006). They can be useful in powering autonomous sensors for long-term operations in less accessible regions. Upflow mode MFCs as shown in Fig. 2.2 D and E are more suitable for wastewater treatment because they are relatively easy to scale-up (He et al., 2005, 2006). On the other hand, fluid recirculation is used in both cases. The energy costs of pumping fluid around are much greater than their power outputs. Therefore, their primary function is not power generation, but rather wastewater treatment. The MFC design in Fig. 2.2 E offers a low internal resistance of 4 Ω because the anode and cathode are in close proximity over a large PEM surface area.

Min and Logan (2004) designed a Flat Plate MFC (FPMFC) with only a single electrode/PEM assembly. Its compact configuration resembles that of a conventional chemical fuel cell. A carbon-cloth cathode that was hot pressed to a Nafion PEM is in contact with a single sheet of carbon paper that serves as an anode to form an electrode/PEM assembly. The FPMFC with two non-conductive polycarbonate plates is bolted together. The PEM links the anodic and the cathodic chambers as shown in Fig. 2.3. The anodic chamber can be fed with wastewater or other organic biomass and dry air can be pumped through the cathodic chamber without any liquid catholyte, both in a continuous flow mode (Min and Logan, 2004).

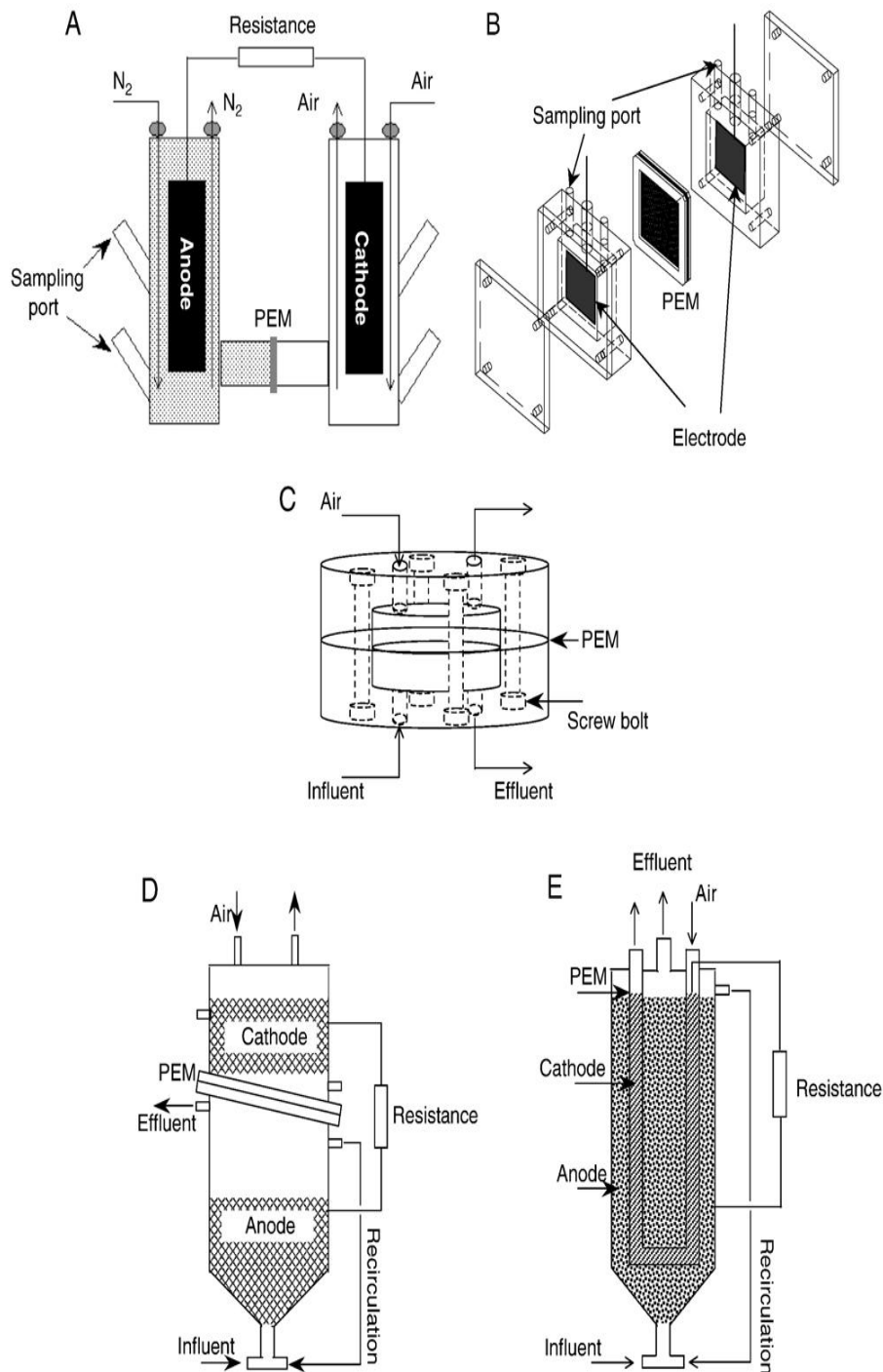


Figure 2.2 : Schematics of a two-compartment MFC in cylindrical shape (A), rectangular shape (B), miniature shape (C), upflow configuration with cylindrical shape (D), cylindrical shape with an U-shaped cathodic compartment (E). (Fig. 2.2A drawn to illustrate a photo in Min et al., 2005a,b. The rest drawn with modifications after Delaney et al., 1984; Allen and Bennetto, 1993; Ringeisen et al., 2006; He et al., 2005, 2006, respectively).

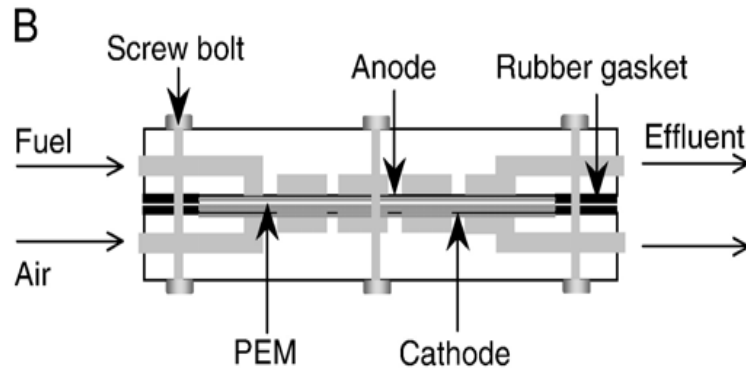


Figure 2.3 : Schematics of side views of a flat plate MFC. (Figures drawn with modifications after Min and Logan, 2004).

2.5.2 Single-compartment MFC systems

Due to their complex designs, two-compartment MFCs are difficult to scale-up even though they can be operated in either batch or continuous mode. One-compartment MFCs offer simpler designs and cost savings. They typically possess only an anodic chamber without the requirement of aeration in a cathodic chamber.

Park and Zeikus (2003) designed a one-compartment MFC consisting of an anode in a rectangular anode chamber coupled with a porous air-cathode that is exposed directly to the air as shown in Fig. 2.2A. Protons are transferred from the anolyte solution to the porous air-cathode (Park and Zeikus, 2003).

Liu and Logan (2004) designed an MFC consisting of an anode placed inside a plastic cylindrical chamber and a cathode placed outside. Fig. 2.2B shows the schematic of a laboratory prototype of the MFC bioreactor. The anode was made of carbon paper without wet proofing. The cathode was either a carbon electrode/PEM assembly fabricated by bonding the PEM directly onto a flexible carbon-cloth electrode, or a stand alone rigid carbon paper without PEM (Liu and Logan, 2004; Liu et al., 2005a; Cheng et al., 2006a).

A tubular MFC system with an outer cathode and an inner anode using graphite granules is shown in Fig. 2.2C (Rabaey et al., 2005b). In the absence of a cathodic chamber, catholyte is supplied to the cathode by dripping an electrolyte over the outer woven graphite mat to keep it from drying up. Rabaey et al. (2005b) pointed out that the use of sustainable, open-air cathodes is critical to practical implementation of such MFCs.

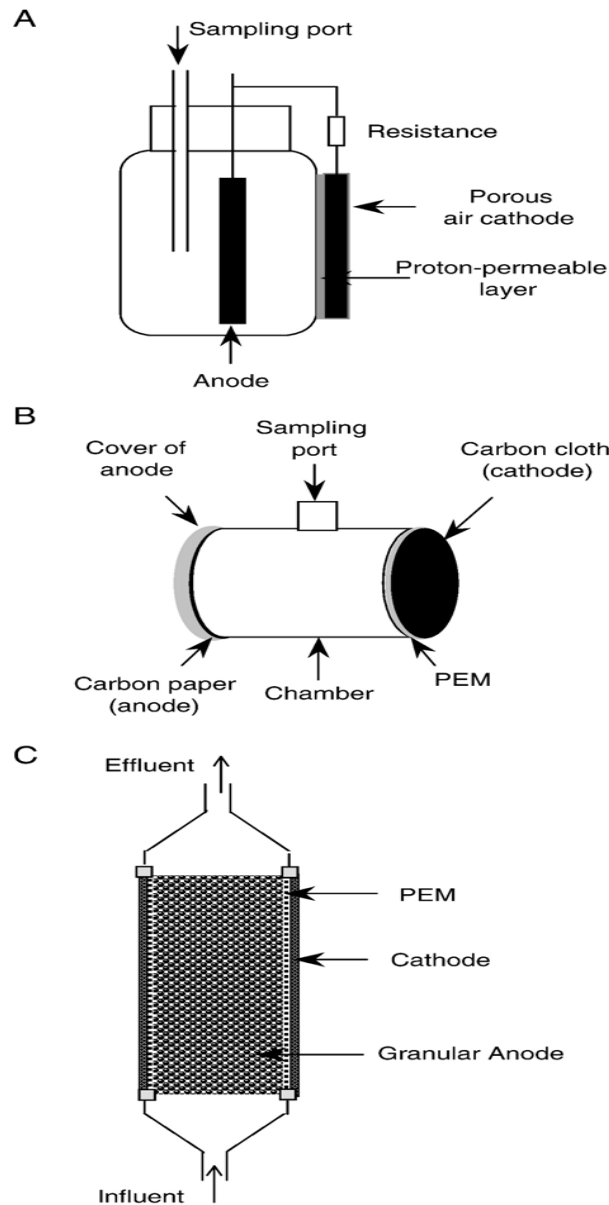


Figure 2.4 : An MFC with a proton permeable layer coating the inside of the window-mounted cathode (A), an MFC consisting of an anode and cathode placed on opposite side in a plastic cylindrical chamber (B), and a tubular MFC with outer cathode and inner anode consisting of graphite granules (C). ((A) drawn to illustrate a photo in Park and Zeikus, 2003. (B) and (C) drawn with modifications after Liu and Logan, 2004; Rabaey et al., 2005b, respectively).

Another type of single-compartment MFC reactor was reported by Liu et al. (2004). Their SCMFC housed both the anode and the cathode in one chamber. It consisted of a single cylindrical Plexiglas chamber with eight graphite rods (anode) in a concentric arrangement surrounding a single cathode as shown in Fig. 2.5. A carbon/platinum catalyst/proton Exchange membrane layer was fused to a plastic support tube to form the air-porous cathode in the center (Liu et al., 2004).

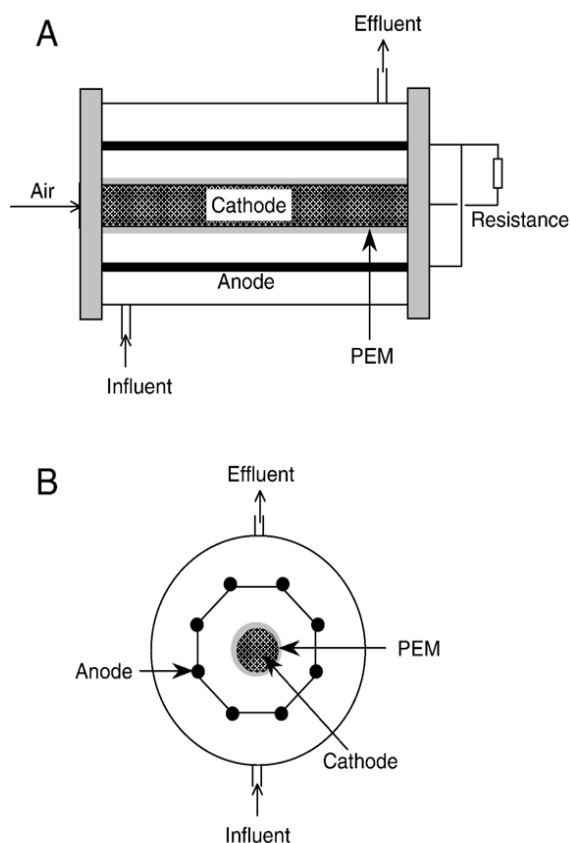


Figure 2.5 : Schematics of a cylindrical SCMFC containing eight graphite rods as an anode in a concentric arrangement surrounding a single cathode. ((A) drawn with modifications after Liu et al., 2004. (B) drawn to illustrate a photo in Liu et al., 2004).

2.5.3 Up-flow mode MFC systems

Jang et al. (2004) provided another design (Fig. 2.6(A)) of an MFC working in continuous flow mode. A Plexiglas cylinder was partitioned into two sections by glass wool and glass bead layers. These two sections served as anodic and cathodic chambers, respectively as shown in Fig. 2.6(A). The disk-shaped graphite felt anode and cathode were placed at the bottom and the top of the reactor, respectively. Fig. 2.6(B) shows another MFC design inspired by the same general idea shown in Fig. 2.6(A) but with a rectangular container and without a physical separation achieved by using glass wool and glass beads (Tartakovsky and Guiot, 2006). The feed stream is supplied to the bottom of the anode and the effluent passes through the cathodic chamber and exits at the top continuously (Jang et al., 2004; Moon et al., 2005). There are no separate anolyte and catholyte. And the diffusion barriers between the anode and cathode provide a dissolved oxygen (DO) gradient for proper operation of the MFCs.

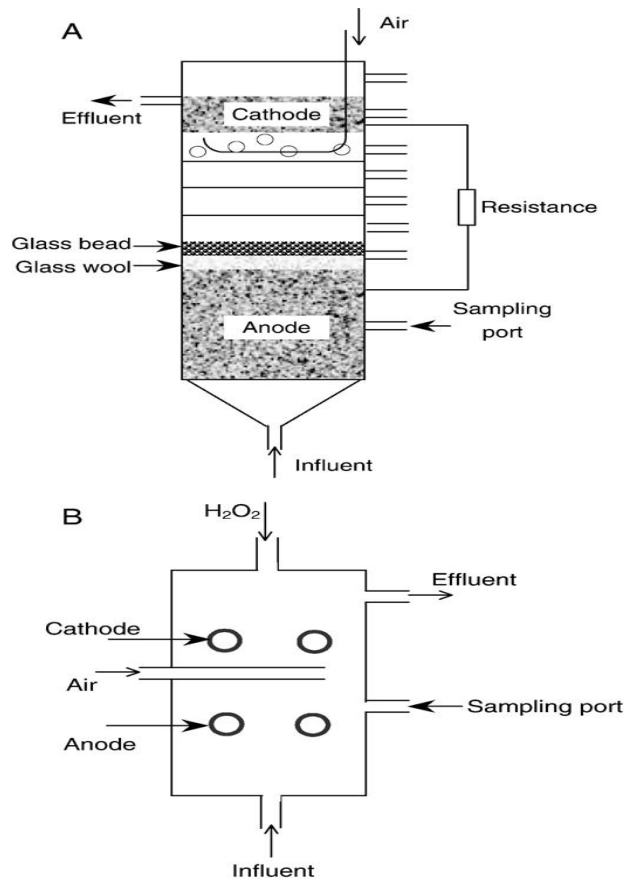


Figure 2.6 : Schematics of mediator- and membrane-less MFC with cylindrical shape (A), and with rectangular shape (B). (Figures drawn with modifications after Jang et al., 2004; Tartakovsky and Guiot, 2006, respectively).

2.5.4 Stacked microbial fuel cell

A stacked MFC is shown in Fig. 2.7. for the investigation of performances of several MFCs connected in series and in parallel (Aelterman et al., 2006). Enhanced voltage or current output can be achieved by connecting several MFCs in series or in parallel. No obvious adverse effect on the maximum power output per MFC unit was observed. Coulombic efficiencies (In fact it is not real Coulombic efficiency but Coulombic percent conversion. Coulombic efficiency describes how much of the electrons can be abstracted from the electron-rich substrates via the electrodes. It is not a measurement of electron transfer rate, while the authors described how much substrate was used for electricity generation before the stream flowed out of the MFCs or MFC stacks differed greatly in the two arrangements with the parallel connection giving about an efficiency six times higher when both the series were operated at the same volumetric flow rate. The parallel-connected stack has higher short circuit current than the series connected stack. This means that higher

maximum bioelectrochemical reaction rate is allowed in the connection of MFCs in parallel than in series. Therefore to maximize chemical oxygen demand removal, a parallel connection is preferred if the MFC units are not independently operated (Aelterman et al., 2006).

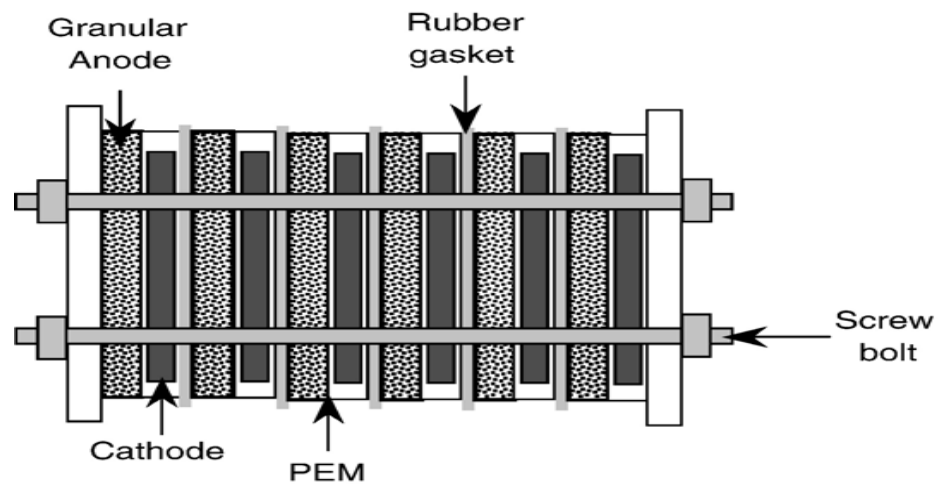


Figure 2.7 : Stacked MFCs consisting of six individual units with granular graphite anode. (Figure drawn to illustrate a photo in Aelterman et al., 2006).

2.6 Performance of Microbial Fuel cell

2.6.1 Ideal performance of MFC

The ideal performance of an MFC depends on the electrochemical reactions that occur between the organic substrate at a low potential such as glucose and the final electron acceptor with a high potential, such as oxygen (Rabaey and Verstrate, 2005). However, its ideal cell voltage is uncertain because the electrons are transferred to the anode from the organic substrate through a complex respiratory chain that varies from microbe to microbe and even for the same microbe when growth conditions differ. Though the respiratory chain is still poorly understood, the key anodic reaction that determines the voltage is between the reduced redox potential of the mediator (if one is employed) or the final cytochrome in the system for the electrophile/anodophile if this has conducting pili, and the anode. For those bacterial species that are incapable of releasing electrons to the anode directly, a redox mediator is needed to transfer the electrons directly to the anode (Stirling et al., 1983; Bennetto, 1984). In such a case the final anodic reaction is that the anode gains the electrons from the reduced mediator.

In mediator-less MFCs utilizing anodophiles such as *G. sulfurreducens* and *R. ferrireducens*, microbes form a biofilm on the anode surface and use the anode as their end terminal electron acceptor in their anaerobic respiration. The anodic potential can be evaluated by the ratio of the final cytochrome of the chain in reduced and oxidized states. The electrode reactions for various types of MFCs and their corresponding redox potentials of those substrates involved in electrode reactions are presented in Table 2 (Hernandez and Newman, 2001; Straub et al., 2001; Rabaey and Verstraete, 2005; Madigan, 2000). The ideal potentials of MFCs can be calculated by the Nernst equation for these reactions and they range from several hundred mV to over 1000 mV.

2.6.2 Actual performance of MFC

The actual cell potential is always lower than its equilibrium potential because of irreversible losses. Activation polarization is attributed to an activation energy that must be overcome by the reacting species. It is a limiting step when the rate of an electrochemical reaction at an electrode surface is controlled by slow reaction kinetics. Processes involving adsorption of reactant species, transfer of electrons across the doublelayer cell membrane, desorption of product species, and the physical nature of the electrode surface all contribute to the activation polarization. For those microbes that do not readily release electrons to the anode, activation polarization is an energy barrier that can be overcome by adding mediators. In mediator-less MFCs, activation polarization is lowered due to conducting pili. Cathodic reaction also faces activation polarization. For example, platinum is preferred over a graphite cathode for performance purpose because it has a lower energy barrier in the cathodic oxygen reaction that produces water. Usually activation polarization is dominant at a low current density. The electronic barriers at the anode and the cathode must be overcome before current and ions can flow (Appleby and Foulkes, 1989).

The resistance to the flow of ions in electrolytes and the electron flow between the electrodes cause Ohmic losses. Ohmic loss in electrolytes is dominant and it can be reduced by shortening the distance between the two electrodes and by increasing the ionic conductivity of the electrolytes (Cheng et al., 2006b). PEMs produce a transmembrane potential difference that also constitutes a major resistance. Concentration polarization is a loss of potential due to the inability to maintain the

initial substrate concentration in the bulk fluid. Slow mass transfer rates for reactants and products are often to blame. Cathodic overpotential caused by a lack of DO for the cathodic reaction still limits the power density output of some MFCs (Oh et al., 2004).

A good MFC bioreactor should minimize concentration polarization by enhancing mass transfer. Stirring and/or bubbling can reduce the concentration gradient in an MFC. However, stirring and bubbling requires pumps and their energy requirements are usually greater than the outputs from the MFC. Therefore, balance between the power output and the energy consumption by MFC operation should be carefully considered. A polarization curve analysis (Rhoads et al., 2005) of an MFC can indicate to what extent the various losses contribute to the overall potential drop. This can point to possible measures to minimize them in order to approach the ideal potential. These measures may include selection of microbes and modifications to MFC configurations such as improvement in electrode structures, better electrocatalysts, more conductive electrolyte, and short spacing between electrodes. For a given MFC system, it is also possible to improve the cell performance by adjusting operating conditions (Gil et al., 2003).

2.7 Effects of Operation Conditions

So far, performances of laboratory MFCs are still much lower than the ideal performance. There may be several possible reasons. Power generation of an MFC is affected by many factors including microbe type, fuel biomass type and concentration, ionic strength, pH, temperature, and reactor configuration (Liu et al., 2005b). With a given MFC system, the following operating parameters can be regulated to decrease the polarizations in order to enhance the performance of an MFC.

2.7.1 Effect of electrode materials

Using better performing electrode materials can improve the performance of an MFC because different anode materials result in different activation polarization losses. Pt and Pt black electrodes are superior to graphite, graphite felt and carbon-cloth electrodes for both anode and cathode constructions, but their costs are much higher. Schroder et al. (2003) reported that a current of 2–4 mA could be achieved with

platinized carbon-cloth anode in an agitated anaerobic culture of *E. coli* using a standard glucose medium at 0.55 mmol/L, while no microbially facilitated current flow is observed with the unmodified carbon-cloth with the same operating conditions. Pt also has a higher catalytic activity with regard to oxygen than graphite materials. MFCs with Pt or Pt-coated cathodes yielded higher power densities than those with graphite or graphite felt cathodes (Oh et al., 2004; Jang et al., 2004; Moon et al., 2006).

Electrode modification is actively investigated by several research groups to improve MFC performances. Park and Zeikus (2002, 2003) reported an increase of 100-folds in current output by using NR-woven graphite and Mn(IV) graphite anode compared to the woven graphite anode alone. NR and Mn(IV) served as mediators in their MFC reactors. Doping ions such as Fe (III) and/or Mn(IV) in the cathode also catalyze the cathodic reactions resulting in improved electricity generations. The principle for their catalytic activity is the same as that of electron shuttles. The electron driving force generated is coupled to the quantivalence change cycles of Fe(III)-Fe(II)-Fe(III) or Mn(IV)-Mn (III) or Mn(II)-Mn(IV) on the cathode. Four times higher current can be achieved with the combination of Mn(IV)-graphite anode and Fe³⁺ graphite cathode compared to plain graphite electrodes (Park and Zeikus, 1999, 2000, 2003). One drawback of using Pt or Pt black electrodes is that their activities are reduced by the formation of a PtO layer at the electrode surface at positive potentials.

Cathode reaction has a Monod-type kinetic relationship with the dissolved oxygen concentration (Oh et al., 2004; Pham et al., 2004). Iron(II) phthalocyanine and cobalt tetramethoxyphenylporphyrin based oxygen cathodes are inexpensive and are efficient alternatives for use in MFCs because they demonstrate similar performances as Pt oxygen electrodes (Zhao et al., 2005, 2006). Catalysts such as Pt, CoTMPP, Mn(IV) and Fe(III) deposited on an air-cathode improve power output by increasing their affinity for oxygen and decreasing the activation energy of the cathodic reaction that reduces O₂ to H₂O (Cheng et al., 2006c).

Some people tend to think that a large cathodic surface area would facilitate electrode reactions on the cathode's surface. However, it was reported that different cathode surface areas had only a small effect on internal resistance and the power output (Oh and Logan, 2006; Oh et al., 2004).

2.7.2 pH buffer and electrolyte

If no buffer solution is used in a working MFC, there will be an obvious pH difference between the anodic and cathodic chambers, though theoretically there will be no pH shift when the reaction rate of protons, electrons and oxygen at the cathode equals the production rate of protons at the anode. The PEM causes transport barrier to the cross membrane diffusion of the protons, and proton transport through the membrane is slower than its production rate in the anode and its consumption rate in the cathode chambers at initial stage of MFC operation thus brings a pH difference (Gil et al., 2003). However, the pH difference increases the driving force of the proton diffusion from the anode to the cathode chamber and finally a dynamic equilibrium forms. Some protons generated with the biodegradation of the organic substrate transferred to the cathodic chamber are able to react with the dissolved oxygen while some protons are accumulated in the anodic chamber when they do not transfer across the PEM or salt bridge quickly enough to the cathodic chamber. Gil et al. (2003) detected a pH difference of 4.1 (9.5 at cathode and 5.4 in anode) after 5-hour operations with an initial pH of 7 without buffering. With the addition of a phosphate buffer (pH 7.0), pH shifts at the cathode and anode were both less than 0.5 unit and the current output was increased about 1 to 2 folds. It was possible that the buffer compensated the slow proton transport rate and improved the proton availability for the cathodic reaction. Jang et al. (2004) supplied an HCl solution to the cathode and found that the current output increased by about one fold. This again suggests that the proton availability to the cathode is a limiting factor in electricity generation. Increasing ionic strength by adding NaCl to MFCs also improved the power output (Jang et al., 2004; Liu et al., 2005b), possibly due to the fact that NaCl enhanced the conductivity of both the anolyte and the catholyte.

2.7.3 Proton exchange system

Proton exchange system can affect an MFC system's internal resistance and concentration polarization loss and they in turn influence the power output of the MFC. Nafion (DuPont, Wilmington, Delaware) is most popular because of its highly selective permeability of protons. Despite attempts by researchers to look for less expensive and more durable substitutes, Nafion is still the best choice. However, side effect of other cations transport is unavoidable during the MFC operation even with Nafion. In a batch accumulative system, for example, transportation of cation species

other than protons by Nafion dominates the charge balance between the anodic and cathodic chambers because concentrations of Na^+ , K^+ , NH_4^+ , Ca^{2+} , Mg^{2+} are much higher than the proton concentrations in the anolyte and catholyte (Rozendal et al., 2006). In this sense, Nafion as well as other PEMs used in the MFCs are not a necessarily proton specific membranes but actually cation specific membranes.

The ratio of PEM surface area to system volume is important for the power output. The PEM surface area has a large impact on maximum power output if the power output is below a critical threshold. The MFC internal resistance decreases with the increase of PEM surface area over a relatively large range (Oh and Logan, 2006).

2.7.4 Operating conditions in the anodic chamber

Fuel type, concentration and feed rate are important factors that impact the performance of an MFC. With a given microbe or microbial consortium, power density varies greatly using different fuels. Many systems have shown that electricity generation is dependent on fuel concentration both in batch and continuous-flow mode MFCs. Usually a higher fuel concentration yields a higher power output in a wide concentration range.

Park and Zeikus (2002) reported that a higher current level was achieved with lactate (fuel) concentration increased until it was in excess at 200 mM in a single-compartment MFC inoculated with *S. putrefaciens*.

Moon et al. (2006) investigated the effects of fuel concentration on the performance of an MFC. Their study also showed that the power density was increased with the increase in fuel concentration.

Gil et al. (2003) found that the current increased with a wastewater concentration up to 50 mg/L in their MFC. Interestingly, the electricity generation in an MFC often peaks at a relatively low level of feed rate before heading downward. This may be because a high feed rate promoted the growth of fermentative bacteria faster than those of the electrochemically active bacteria in a mixed culture (Moon et al., 2006; Kim et al., 2004; Rabaey et al., 2003). However, if microbes are growing around the electrodes as biofilms, the increased feed rate is unlikely to affect the flora. One possible reason is that the high feed rate brings in other alternate electron acceptors competing with the anode to lower the output.

2.7.5 Operating conditions in the cathodic chamber

Oxygen is the most commonly used electron acceptor in MFCs for the cathodic reaction. Power output of an MFC strongly depends on the concentration level of electron acceptors. Several studies (Oh et al., 2004; Pham et al., 2004; Gil et al., 2003) indicated that DO was a major limiting factor when it remained below the air-saturated level. Surprisingly, a catholyte sparged with pure oxygen that gave 38 mg/L DO did not further increase the power output compared to that of the air-saturated water (at 7.9 mg/L DO) (Oh et al., 2004; Min and Logan, 2004; Pham et al., 2004;). Rate of oxygen diffusion toward the anode chamber goes up with the DO concentration. Thus, part of the substrate is consumed directly by the oxygen instead of transferring the electrons through the electrode and the circuit (Pham et al., 2004). Power output is much greater using ferricyanide as the electron acceptor in the cathodic chamber. So far, reported cases with very high power outputs such as 7200 mW/m², 4310 mW/m² and 3600 mW/m² all used ferricyanide in the cathodic chamber (Oh et al., 2004; Schroder et al., 2003; Rabaey et al., 2003, 2004), while less than 1000 mW/m² was reported in studies using DO regardless of the electrode material. This is likely due to the greater mass transfer rate and lower activation energy for the cathodic reaction offered by ferricyanide (Oh et al., 2004). Using hydrogen peroxide solution as the final electron acceptor in the cathodic chamber increased power output and current density according to Tartakovsky and Guiot (2006). As a consequence, aeration is no longer needed for single compartment MFCs with a cathode that is directly exposed to air. Rhoads et al. (2005) measured the cathodic polarization curves for oxygen and manganese and found that reducing manganese oxides delivered a current density up to 2 orders of magnitude higher than that by reducing oxygen.

Surely changing operating conditions can improve the power output level of the MFCs. However, it is not a revolutionary method to upgrade the MFCs from low power system to a applicable energy source at the very present. The bottleneck lies in the low rate of metabolism of the microbes in the MFCs. Even at their fastest growth rate (i.e. μ_{\max} value) microbes are relatively slow transformers. The biotransformation rate of substrates to electrons has a fixed ceiling which is inherently slow. Effort should be focused on how to break the inherent metabolic limitation of the microbes for the MFC application. High temperature can accelerate

nearly all kinds of reactions including chemical and biological ones. Use of thermophilic species might benefit for improving rates of electron production, however, to the best of our knowledge, no such investigation is reported in the literature. Therefore this is probably another scope of improvement for theMFC technology from the laboratory research to a real applicable energy source.

3. MATERIALS AND METHODS

The preliminary works, acclimation period and start-up period of MFC experiments, and the experiments with varying influent organic matter concentrations were done to study the production of electricity and the oxidation of the pollutants contained in a synthetic wastewater fed with sodium acetate as carbon sources.

3.1 The Preliminary Work for the Setup of the MFC System

3.1.1 Acclimation period

Activated sludge was taken from Bahçeşehir Domestic Wastewater Treatment Plant and fed with aerated tap water and sodium acetate solution mixture in an aerated fill and draw reactor. The glass reactor which has an effective volume of 4 L was used. Figure 3.1 shows the acclimation reactor.



Figure 3.1 : The acclimation reactor.

The hydraulic detention time was set at one day, and the aeration of the reactor was withdrawn after 23 hours to allow one hour of settling. The aqueous upper portion of the reactor was wasted and the reactor was filled with aerated tap water and fed with sodium acetate solution. The sodium acetate solution was prepared weekly to have a COD concentrations of 400 mg/l in the reactor.

After the mixed liquor MLVSS concentration reached at the desired level of 2000 mg/l, the daily MLVSS concentrations were measured and the amount of excess sludge produced, was wasted. When the amount of excess sludge was approximately constant, the fill and draw system is said to reach steady-state at a constant F/M ratio with definite sludge age of 20days, F/M ratio and constant daily COD removal efficiency.

3.1.2 Start-up period of MF

3.1.2.1 MFC Design

The constructed microbial fuel cell system consists of the following units:

1. Reactor (Anode and Cathode Chambers)
2. Proton Exchange Membrane (Nafion 117)
3. Electrodes (Chrome-Nickel Plate)
4. Stirrer
5. Air Pump
6. Multimeter
7. Computer

As mentioned above, the materials which are necessary for the start-up period of the microbial fuel cell are shown in Figure 3.2.

Microbial fuel cell was operated in fill and draw mode at room temperature.

As seen in Fig. 3.3, the two-chamber MFC was consisted of Plexiglass chamber (15cm×15cm×15 cm) with a proton exchange membrane (Nafion 117) which separates reactor into parts. Volume of the anode and cathode chambers were the same, about 2.5 L.

The electrode made by chrome-nickel was put in both sides of the reactor. The surface areas of the anode and cathode were the same, about 225 cm².

Voltage was measured using a multimeter (UT60F) and a data acquisition system, which can continuously monitor the voltage and transfer data to the computer at an interval of 5 min.



Figure 3.2 : Materials which are necessary for the start-up period of the microbial fuel.



Figure 3.3 : Experimental set up of microbial fuel cell.

3.1.2.2 Set-up and start-up operation of the system

In the set-up period, connections and placements of materials were done in eleven steps. These steps can be classified as following:

1. A reactor was separated into two parts which are anodic and cathodic chambers was constructed.
2. Proton exchange membrane, Nafion 117 , was cut and put in distilled water for two hours to obtain expanded shape.
3. Nafion was compressed between two binders which was made from plexyglass
4. Nafion membrane was placed between anode and cathode chamber.
5. The volumes of the chambers were measured and marked.
6. The electrode which has a black wiring was put in the anode chamber.
7. The electrode which has a red wiring was put in the cathodic chamber.
8. Stirrer was placed in the bottom of the anodic part of MFC.
9. The two diffusers were placed in the cathodic chamber.
10. Multimeter was connected to the red and black wires to complete the circuit.
11. The connection between the computer and multimeter was done for continuous data storage.

After setup of the system the anodic chamber was seeded with sodium acetate acclimated activated sludge, by using biomass of about 1000 mg/l VSS to start-up the MFC system. Tap water was added to the cathodic chamber and the air was supplied to this chamber. Stirrer was turned on. After the nutrient solutions were added on the biomass, the cathodic chamber was fed with synthetic wastewater (sodium acetate solution).

In this period, soluble COD and voltage profiles of the system was observed for a period long enough to ensure the depletion of the substrate.

3.2 Analysis Conducted and Calculated Parameters in the MFC System

After start-up period, the anodic chamber of the microbial fuel cell was fed with different concentrations of sodium acetate solution, respectively 325 mg/l, 160 mg/l and 650 mg/l COD, for three different periods. The aerobic cathodic chamber was not stirred and was aerated with a sufficiently small flow rate of air, to prevent the crossover of the oxygen from the cathodic to the anodic chamber. This chamber only contained tap water.

The experiments were done to observe COD reduction, biomass generation and electricity production. pH was also monitored during the experiments. Chemical oxygen demand and volatile suspended solid were measured in duplicates using standard methods. pH was measured using a pH meter.

Calculation procedures for electricity production consisted of seven steps.

Step 1: The voltage can be defined as a function of the external resistance, or load on the circuit, and the current. Voltage yielded from MFC for long time operation was recorded automatically by a computer at an interval of five minutes.

The highest voltage produced in an MFC is the open circuit voltage (OCV) which was measured with the circuit disconnected (infinite resistance, zero current). OCV was determined for different sodium acetate concentrations.

Step 2: After determination of OCV a 1000 Ω external resistance was connected to the MFC.

The current produced in MFC was small, so the current was not measured, but instead it was calculated according to Ohm's law:

$$I_{MFC} = \frac{V_{1000\Omega}}{1000\Omega} \quad (3.1)$$

where $V_{1000\Omega}$ (V) is the measured voltage, I_{MFC} (A) is the current, and 1000Ω is the external resistance.

Step 3: To make MFCs useful as a method to generate power, it was essential to optimize the system for power production. Power was calculated from voltage and current as:

$$P = I.V \quad (3.2)$$

The power output by MFC was calculated from the measured voltage across the load and the current as:

$$P = I_{MFC} \cdot V_{MFC} \quad (3.3)$$

where P (Watt) is the power, I_{MFC} (A) is the calculated current, and V_{MFC} (V) is the measured voltage.

Step 4: As with any power source, the objective was to maximize power output and therefore to obtain the highest current density under conditions of the maximum potential. Current density was calculated as

$$I_{AN} = \frac{I_{MFC}}{A_{anode}} \quad (3.4)$$

where I_{AN} (A.cm⁻²) is the anodic current density, I_{MFC} (A) is the calculated current, A_{anode} (cm²) is the surface area of the used electrode in the anode chamber.

Step 5: Knowing how much power is generated by an MFC does not sufficiently describe how efficiently that power is generated by the specific system architecture. For example, the amount of anode surface area available for microbes to grow on can affect the amount of power generated. Thus, it is common to normalize power production by the surface area of the anode so that the power density produced by the MFC is given by:

$$P_{AN} = \frac{P}{A_{anode}} \quad (3.5)$$

where P_{AN} (W.cm⁻²) is the power density, P (W) is the calculated power, A_{anode} (cm²) is the surface area of the studied electrode in the anode chamber.

Step 6: Polarization curves in MFC give important information about the operating conditions of the MFC, in particular about the actual capabilities of the MFC. These curves allow discerning three important parameters: the OCV or the maximum allowable MFC voltage (for a nil current), the maximum intensity reachable (for a nil potential) and the maximum feasible current density. Maximum power density and internal resistance of MFCs are obtained by polarization curves. Polarization curves were obtained by varying the external resistance over a range from 1 to 5 kΩ when the voltage output achieved is constant. According to Ohm's law, when the power density is the maximum, the internal and external resistances are equal.

Step 7: While generating power is a main goal of MFC operation, we also seek to extract as much of the electrons stored in the biomass as possible as current, and to recover as much energy as possible from the system. The recovery of electrons is referred to as *Coulombic efficiency* defined as the fraction (or percent) of electrons recovered as current versus the electrons present in the fed organic matter. The oxidation of a substrate occurs with the removal of electrons, with the moles of electrons defined for each substrate based on writing down the half reaction.

The Coulombic efficiency was calculated using the ratio of total Coulombs obtained in the experiment (CP) to the theoretical amount (CT) available from complete substrate oxidation.

$$C_E = \frac{M \cdot I_{MFC} \cdot t}{F \cdot n \cdot V_{anode} \cdot \Delta C} \quad (3.6)$$

Where M (g/mol) is molecular weight of the substrate I_{MFC} (A) represents the calculated current, t (s) is the time interval, F (C/mol) is the Faraday constant (96,485C/mol), n is the number of moles of electrons produced per mol of substrate, V is the volume of anode (L), ΔC is the absolute removal amount of COD (g/L)

Table 3.1 shows the summary of the operating conditions and the parameters investigated during the experiments.

Table 3.1: Summary of the operating conditions and the parameters investigated during the experiments.

STEPS	FEEDING	RESISTANCE	PARAMETER
1	325 mg/1 COD	-	COD removal, MLSS and MLVSS concentration, Voltage, OCV
2	325 mg/1 COD	1 k Ω	COD removal, MLSS and MLVSS concentration, Voltage, Current, Power, Power Density, Current Density
3	325 mg/1 COD	1 k Ω - 5 k Ω	Polarization Curve
4	650 mg/1 COD	-	COD removal, concentration, Voltage, OCV
5	650 mg/1 COD	1 k Ω	COD removal, MLSS and MLVSS concentration, Voltage, Current, Power, Power Density, Current Density
6	650 mg/1 COD	1 k Ω - 5 k Ω	Polarization Curve
7	160 mg/1 COD	-	COD removal, Voltage, OCV
8	160 mg/1 COD	1 k Ω	COD removal, MLSS and MLVSS concentration, Voltage, Current, Power, Power Density, Current Density
9	160 mg/1 COD	1 k Ω - 5 k Ω	Polarization Curve

4. EXPERIMENTAL RESULTS

4.1 The Preliminary Experimental Results

4.1.1 Acclimation period

4.1.1.1 COD profiles

As seen from Figure 4.1, soluble influent and effluent COD profiles were observed for a period long enough, approximately 90 days, to ensure the steady state operation of the system, until the final COD values were constant.

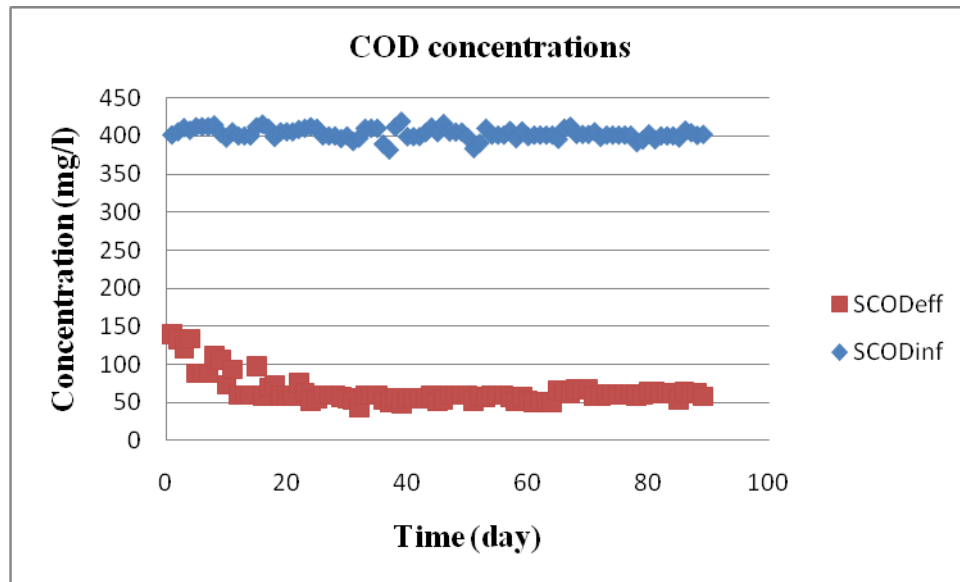


Figure 4.1: Influent and effluent COD concentration in the acclimation reactor.

As seen from Figure 4.2, the COD removal efficiency was approximately between 65-80% for 25 days, after 25 days the COD removal efficiency reached to approximately 86-87% and stayed constant for 2 months.

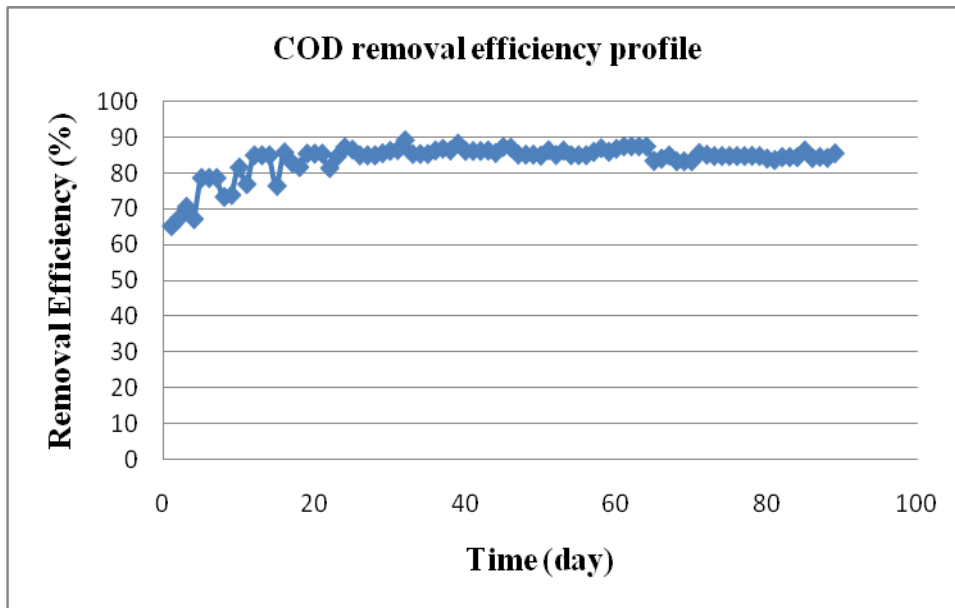


Figure 4.2: COD removal efficiency in the acclimation reactor.

4.1.1.2 MLSS-MLVSS profile

As seen from Figure 4.3, the mixed liquor MLVSS concentration was kept at 2000 mg/L, the daily MLVSS concentrations were observed and the amount of excess sludge wasted was determined as 200 ml/day. When the amount of excess sludge was approximately constant, the fill and draw system is said to reach steady-state with a sludge age of 20 days.

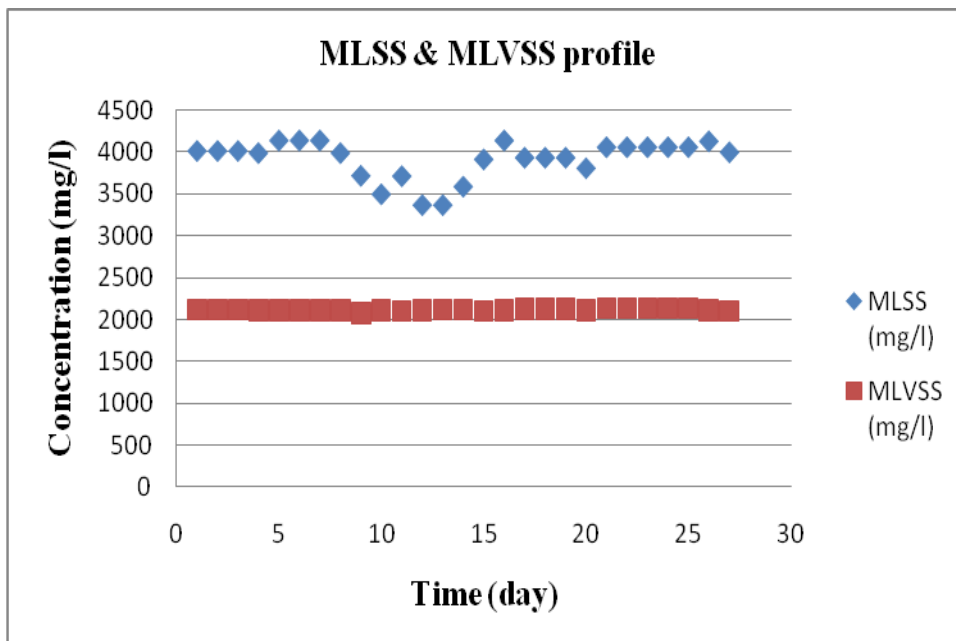


Figure 4.3: MLSS-MLVSS concentrations in the acclimation reactor.

4.1.2 Start-up period results

4.1.2.1 COD profiles

The influent and effluent COD concentrations of the MFC reactor is illustrated in Figure 4.4. As seen from the Figure 4.4, soluble influent and effluent COD profiles were observed for a period long enough, approximately 20 days, to ensure the depletion of the substrate, until the effluent COD values were constant.

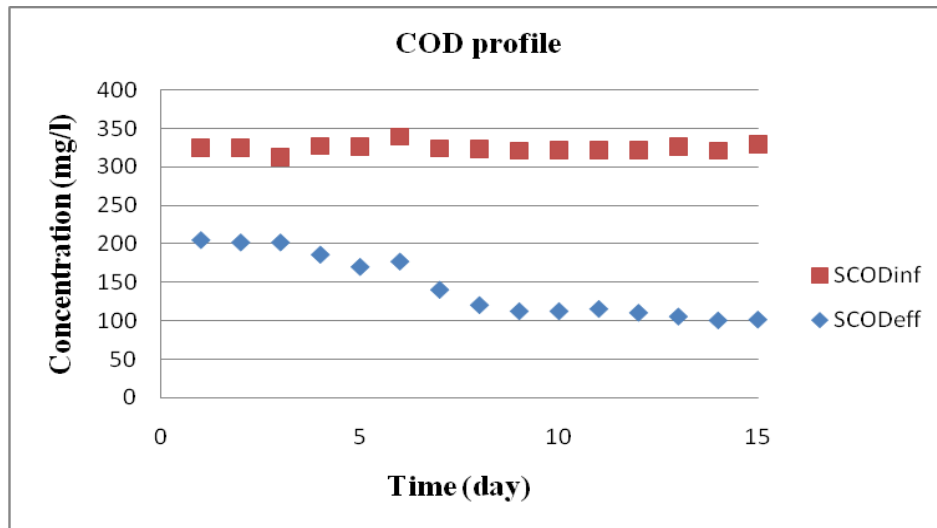


Figure 4.4: Influent and effluent COD concentration in the start-up MFC reactor.

As seen from Figure 4.5, the COD removal efficiency was between 37-56% for 7 days, after 7 days the COD removal efficiency reached to approximately 67-69% and stayed constant for a week.

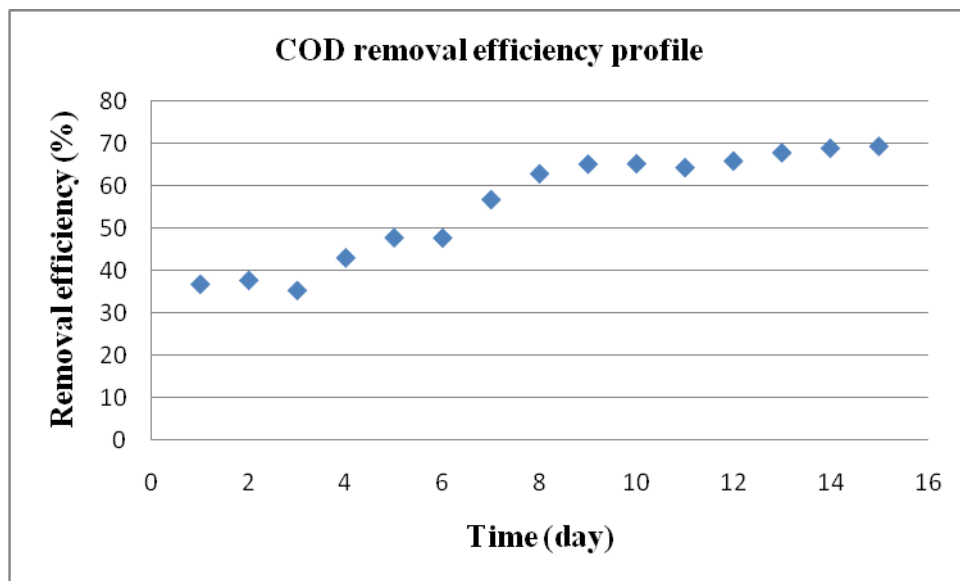


Figure 4.5: COD removal efficiency in the start-up MFC reactor.

4.1.2.2 MLSS-MLVSS profiles

As seen from the Figure 4.6, the mixed liquor MLVSS concentration was started at 1000 mg/L, the daily MLVSS concentrations were observed without wasting sludge and during this period the amount of MLVSS concentration has reached to 3000 mg/l. After 7 days the amount of excess sludge produced was determined as 125ml/day was wasted. When the amount of excess sludge was approximately constant, 1500 mg/l, the MFC system is said to reach steady-state with sludge age of 20 days.

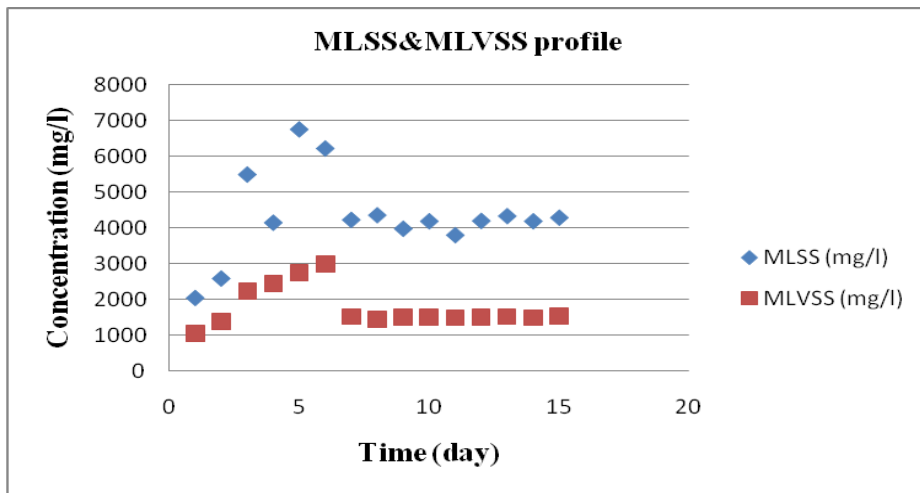


Figure 4.6: MLSS-MLVSS concentrations in the start-up MFC reactor.

4.1.2.3 Electricity generation profile

As seen from Figure 4.7, the electricity generation was started at 0.037 V, the daily voltage changes were observed without wasting sludge and during this period the electricity generation reached to 0.109 V at the end of 7 days. When the COD removal efficiency was approximately constant, the MFC system is said to reach steady-state with an OCV of 0.201V, for start-up period.

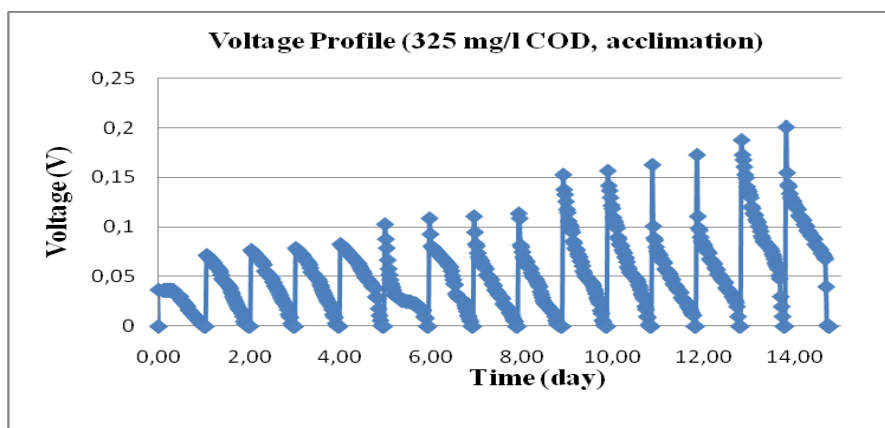


Figure 4.7: Electricity generation in the start-up MFC reactor.

4.2 MFC Experiment Results for Different COD Concentrations

4.2.1 MFC results for 325 mg/l COD concentration without external resistance

The MFC system was operated feeding 325 mg/L COD concentration with the addition of sodium acetate solution. This feeding regime was applied in two steps, which are with suspended biomass and without suspended biomass. The working volume of the anodic chamber was 2.5 L. All the experiments were performed at room temperature of 25°C in a temperature controlled laboratory.

4.2.1.1 COD profiles

4.2.1.1.1 COD profiles without suspended biomass

The first set of experiments were started feeding the system with 325 mgCOD/L sodium acetate solution without suspended biomass (only with attached biomass on the electrode). As seen from Figure 4.8, soluble influent and effluent COD profiles were observed for a 3 day period to see the effect of the suspended biomass for COD removal and electricity generation in MFC system. As seen from the graph, the COD removal efficiency was approximately 78% for the MFC reactor without suspended biomass. Figure 4.9 shows the COD removal for the first 4 hours after feeding the system.

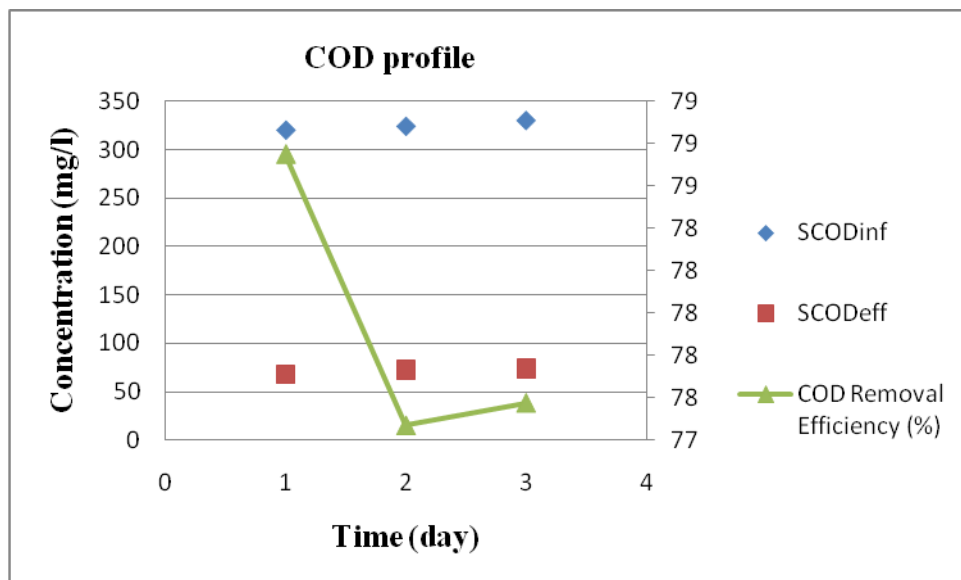


Figure 4.8: Influent and effluent COD concentrations and COD removal efficiencies of the MFC reactor without suspended biomass.

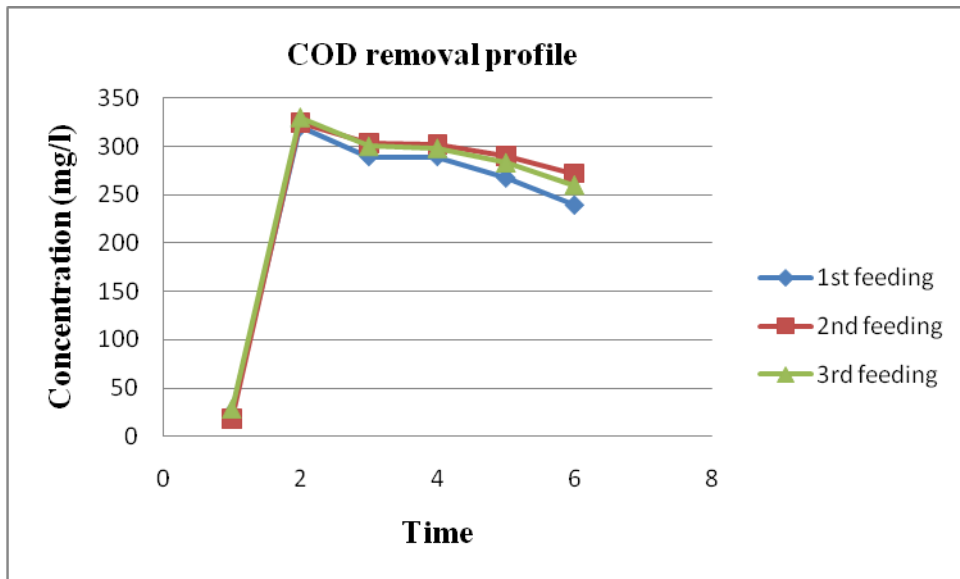


Figure 4.9: COD removal of the MFC reactor without suspended biomass.

4.2.1.1.2 COD profiles with suspended biomass

The second set of experiments were performed feeding the system with 325 mg/l COD sodium acetate solution with suspended biomass. As seen from Figure 4.10, soluble effluent and influent COD profiles were observed for 7 days to ensure the depletion of the substrate in MFC system without resistance. As seen from the graph, the COD removal efficiency was approximately 75% for the MFC reactor with suspended biomass. Figure 4.11 shows the COD removal for the first 4 hours after feeding the system.

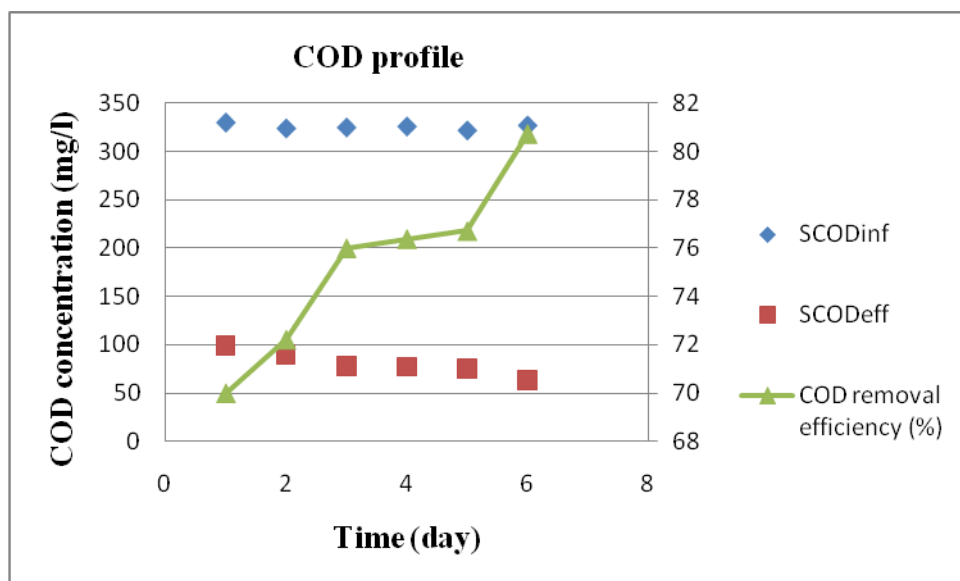


Figure 4.10: Influent and effluent COD concentrations and COD removal efficiencies of the MFC reactor with suspended biomass.

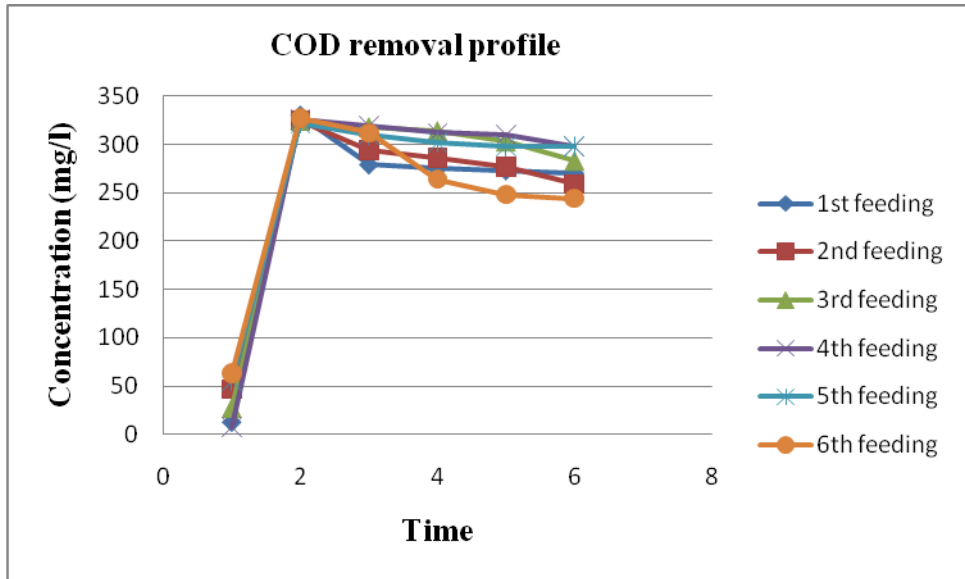


Figure 4.11: COD removal of the MFC reactor with suspended biomass.

4.2.1.2 MLSS and MLVSS profiles

As seen from Figure 4.12, the mixed liquor MLVSS concentration was kept at 1500 mg/L, the daily MLVSS concentrations were observed and the amount of excess sludge produced was determined as 125 ml/day. During this period, the amount of excess sludge was approximately constant, the system is said to be operated at steady-state with a sludge age of 20 days.

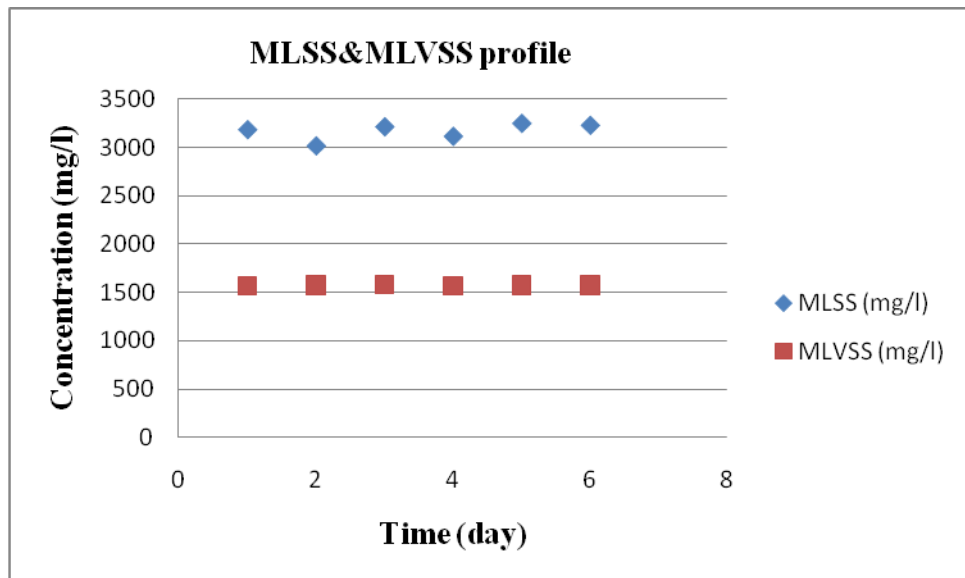


Figure 4.12: MLSS-MLVSS concentrations in the MFC reactor.

4.2.1.3 pH profile

The mixed liquor pH values in the anodic chamber were measured to be between 7-7.09 for the first 3 hours after sodium acetate feeding, as given in Figure 4.13. The

average pH value of the system monitored from time to time always remained in the ranges of 6.99-7.15 throughout the whole cycle.

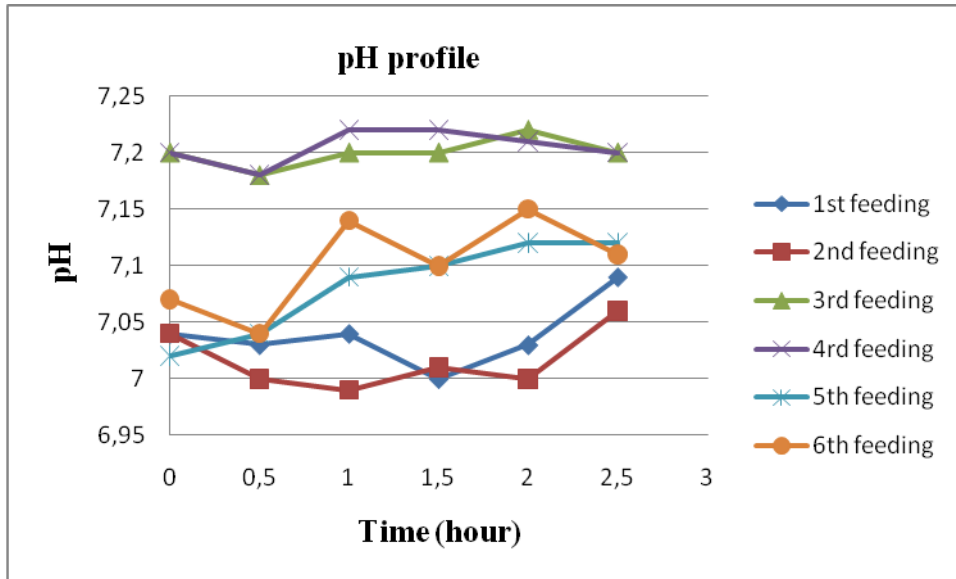


Figure 4.13: pH profiles of the MFC reactor with suspended biomass.

4.2.1.4 Voltage profiles

4.2.1.1.3 Voltage profile without suspended biomass

As seen from Figure 4.14, the electricity generation started at 0.193 V, the daily voltage observed without suspended biomass and during this period the electricity generation was increased to 0.224 V at the end. MFC system without biomass is said to operated with OCV, 0.224 V.

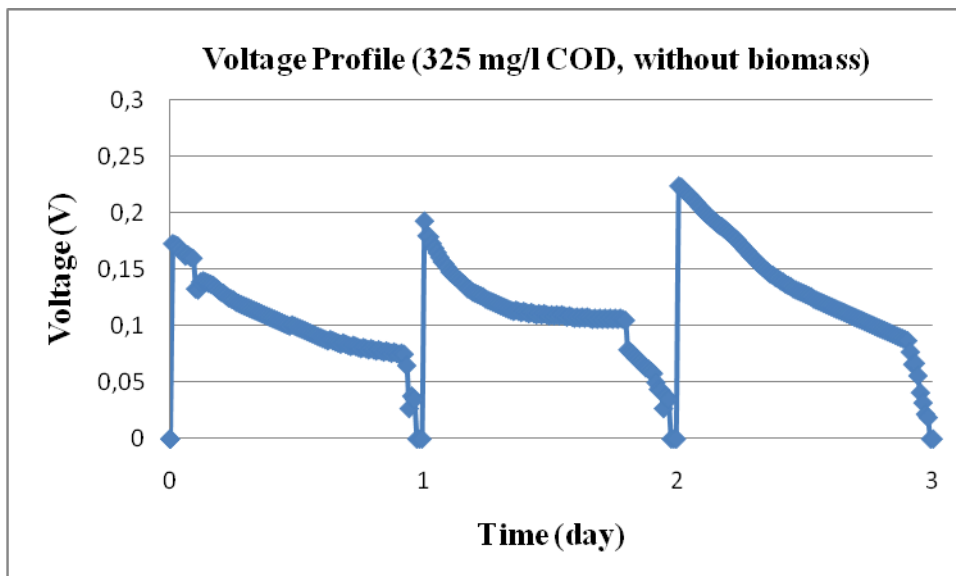


Figure 4.14: Voltage profile without suspended biomass.

4.2.1.1.4 Voltage profile with suspended biomass

As seen from Figure 4.15, the electricity generation was started at 0.178 V, the daily voltage changes were observed with suspended biomass and during this period the electricity generation reached to a maximum of 0.3 V at the end of 7 days. MFC system with biomass is said to operated with an OCV of 0.3 V.

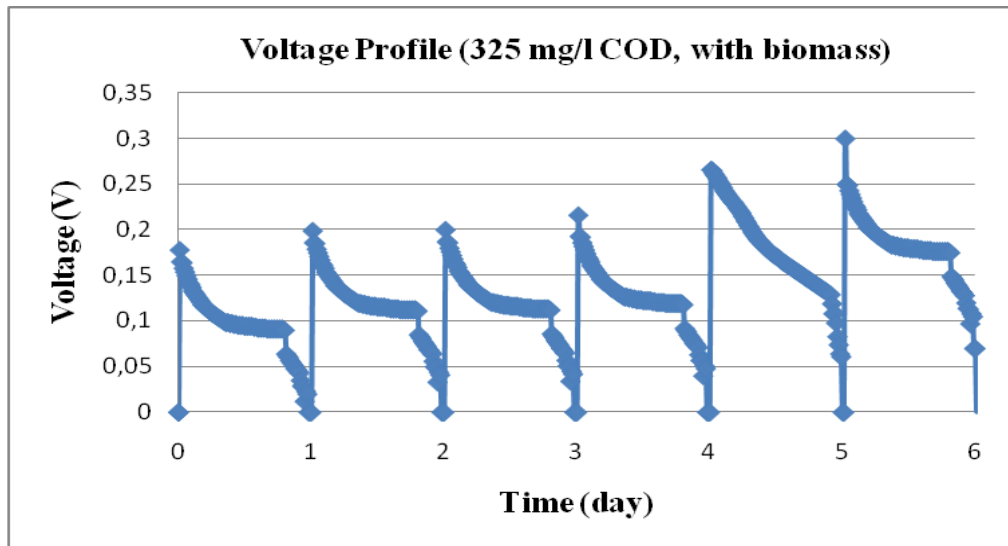


Figure 4.15: Voltage profile with suspended biomass.

4.2.1.5 COD and OCV profile

As seen from Figure 4.16, COD and voltage profiles were observed for a day to ensure the depletion of the substrate and monitor OCV in MFC system without resistance. The system was fed with 325 mg/l COD and COD removal was observed for 10 hours after feeding and also after 22 hours. The system was fed with 20 ml of Solution A and Solution B for nutritional requirements and to provide a buffer capacity and substrate was added after 30 minutes. The COD removal efficiency was approximately 75% in the MFC reactor with biomass. The MFC system fed with sodium acetate was operated with an OCV of 0.3 V.

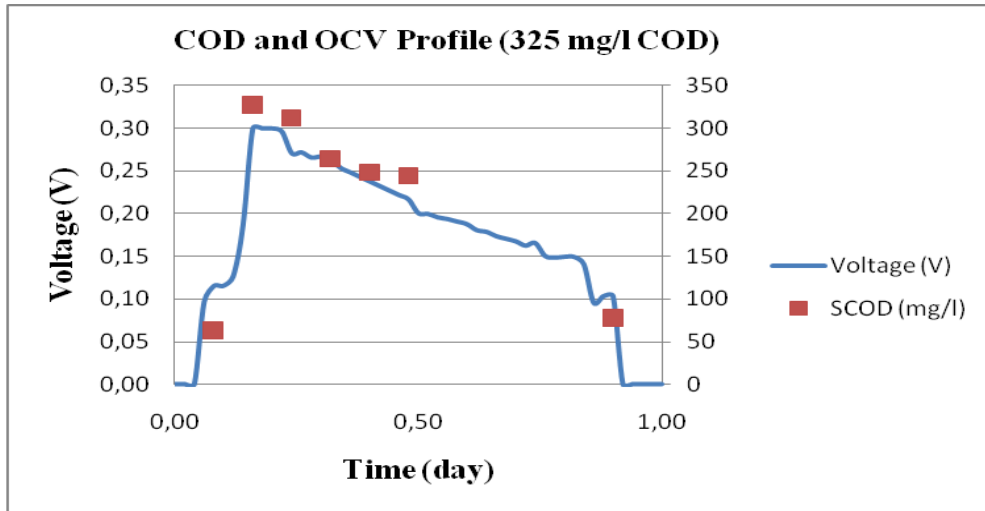


Figure 4.16: COD and OCV profile in the MFC fed with 325 mg/l COD without resistance.

4.2.2 MFC results for 325 mg/l COD concentration with external resistance

4.2.2.1 COD profiles

As seen from Figure 4.17, soluble influent and effluent COD profiles were observed in the MFC system with 1 kΩ external resistance. The system was fed with 325 mg/l COD and COD removal was monitored for 6 days. As seen from the graph, the COD removal efficiency was approximately 78% for a MFC reactor with external resistance.

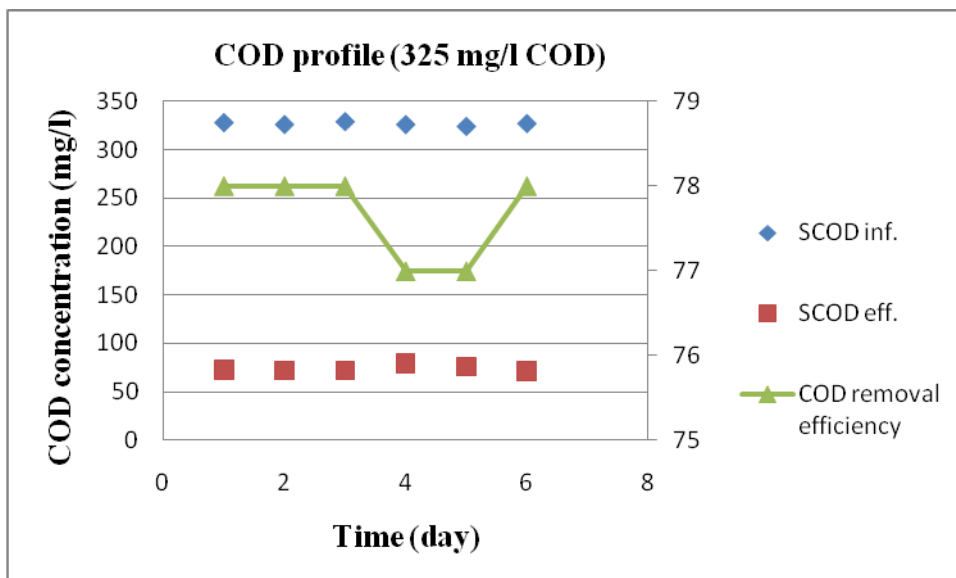


Figure 4.17: Influent and effluent COD concentrations and COD removal efficiencies in the MFC reactor fed with 325 mg/l COD.

As seen from Figure 4.18, COD removal of the system during the first 4 hours after feeding were observed for 6 days in MFC system with 1 k Ω resistance. More than 15% of COD was removed in 1 hour after feeding. The COD removal efficiencies were similar for all cycles.

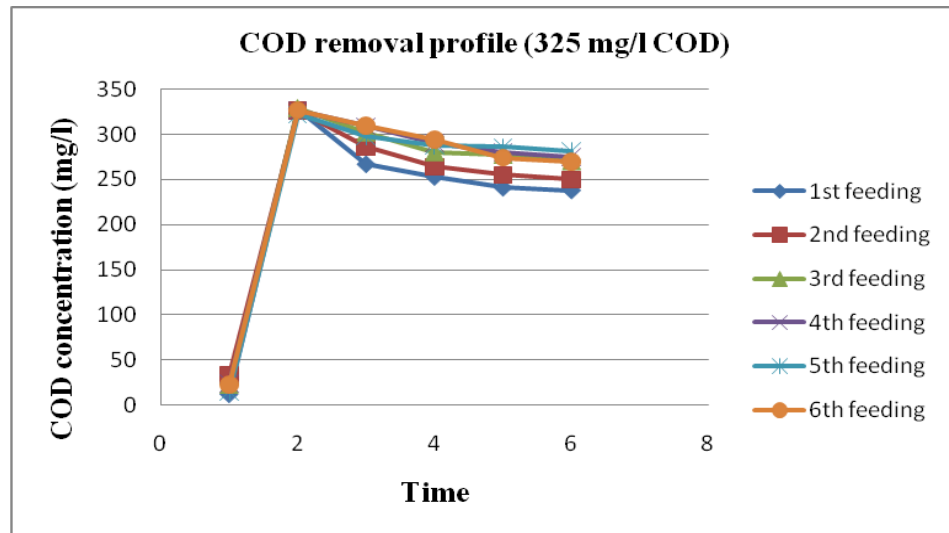


Figure 4.18: COD removal in the MFC reactor fed with 325 mg/l COD.

4.2.2.2 MLSS and MLVSS profiles

As seen from Figure 4.19, the mixed liquor MLVSS concentration was kept at 1500 mg/L, the daily MLVSS concentrations were monitored and the average amount of excess sludge wasted was determined as 125 ml/day. During this period, the amount of excess sludge was approximately constant, the system is said to be operated at steady-state with a sludge age of 20 days.

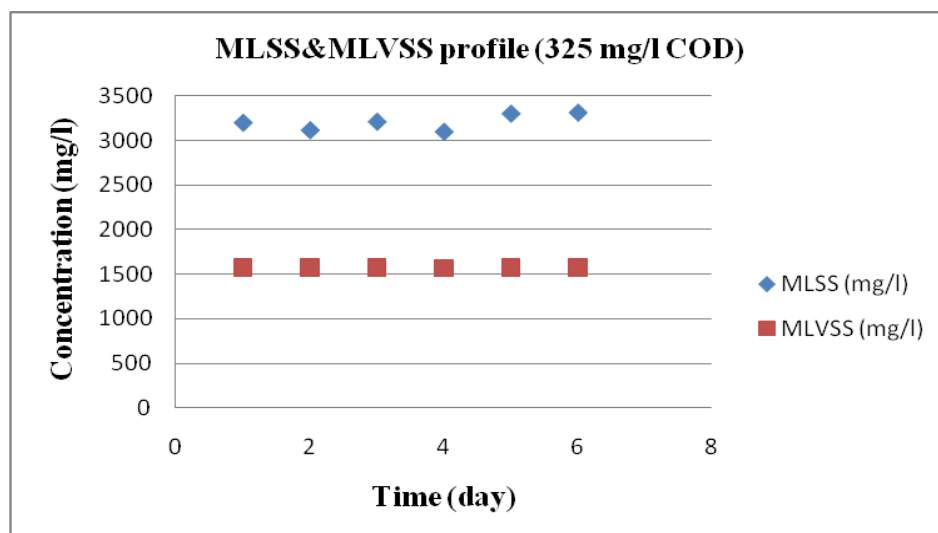


Figure 4.19: MLSS-MLVSS concentrations in the MFC reactor fed with 325 mg/l COD.

4.2.2.3 pH profile

As seen from Figure 4.20, the pH was approximately between 7.00-7.15 during the monitored period. The daily pH was measured and the system was operated at neutral pH.

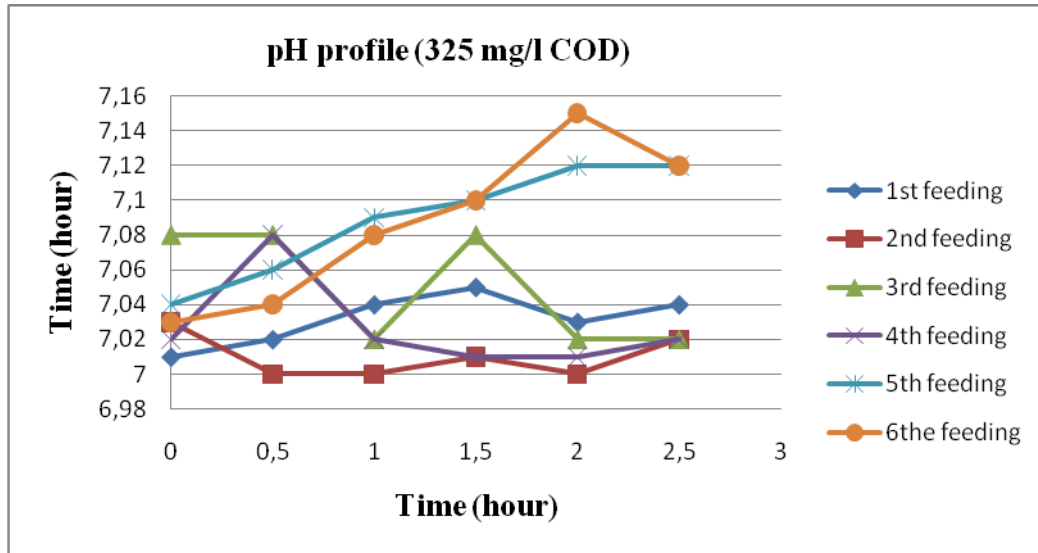


Figure 4.20: pH profiles in the MFC reactor fed with 325 mg/l COD.

4.2.2.4 Voltage profile with suspended biomass and 1 kΩ resistance

As seen from Figure 4.21, the electricity generation in MFC system with 1500 mg/l biomass and 1 kΩ external resistance was 0.2 V on the average for 6 days of operation. The voltage profiles were similar for each cycle.

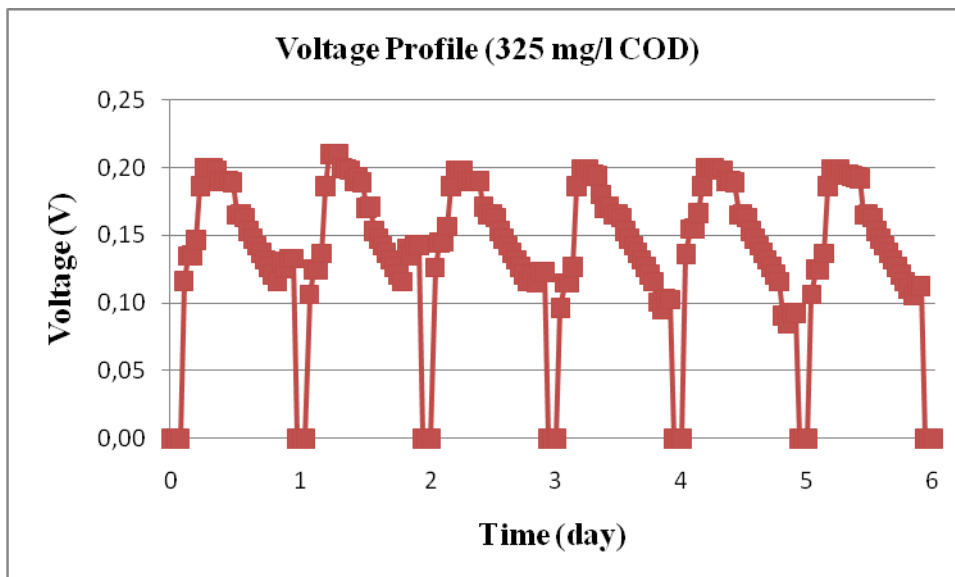


Figure 4.21: Voltage profile in the MFC fed with 325 mg/l COD.

4.2.2.5 Power and current profile

The current and power were calculated as given in Materials and Methods section. As seen from Figure 4.22, the current and power profiles were obtained for 6 days. The average current and power obtained during 6 cycles were 0.2 mA and 40 mW, respectively.

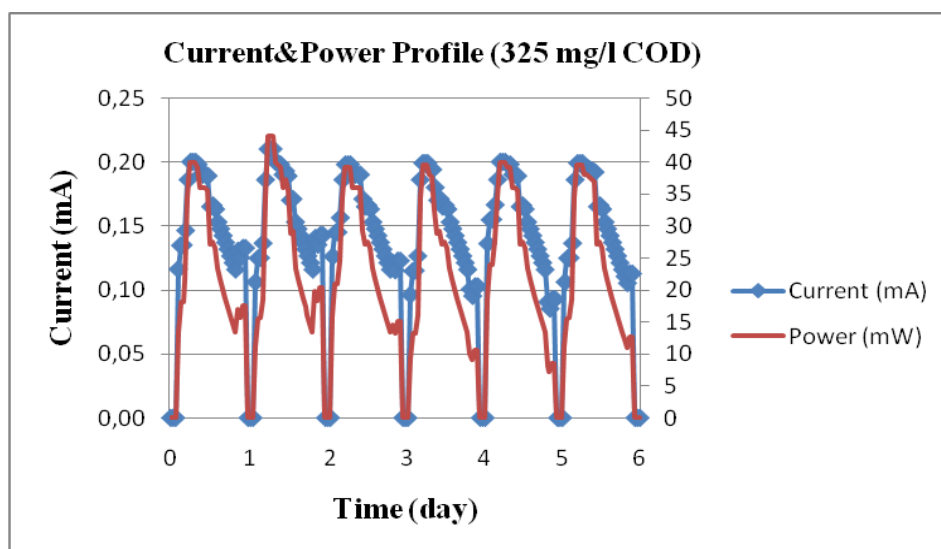


Figure 4.22: Current and power profiles in MFC fed with 325 mg/l COD.

4.2.2.6 Density profiles

The current and power densities were calculated as given in Materials and Methods section. As seen from Figure 4.23, the current and power profiles were obtained for 6 days. The average current and power densities obtained during 6 cycles is $9.3 \text{ mA}\cdot\text{m}^{-2}$ and $1960 \text{ mW}\cdot\text{m}^{-2}$.

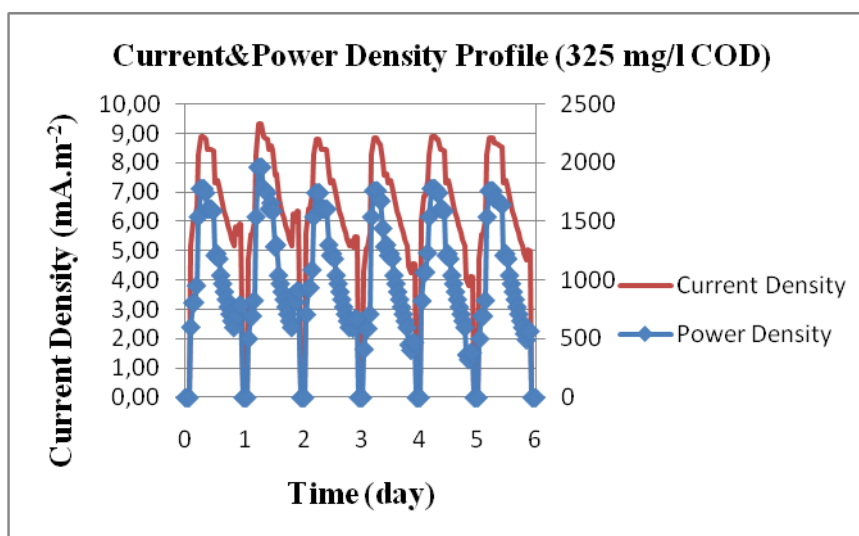


Figure 4.23: Current and power density profiles in MFC fed with 325 mg/l COD.

4.2.2.7 Polarization curve experiment for 325 mg/l COD

The polarization curve was obtained by plotting voltage versus current density with 5 different external resistances ranging from 1k Ω to 5k Ω for 325 mg/l feeding. As seen from Figure 4.24, when voltage increases, the current density decreases. Internal resistance of the system was calculated from the slope of the curve.

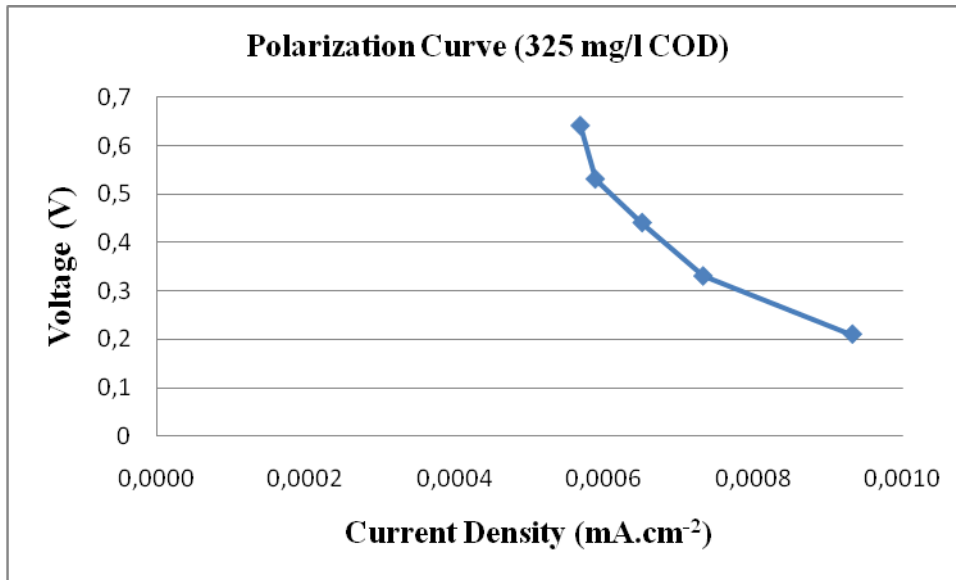


Figure 4.24: Polarization curve in the MFC fed with 325 mg/l COD.

4.2.3 MFC results for 650 mg/l COD concentration without external resistance

4.2.3.1 Voltage and COD profile

As seen from Figure 4.25, COD and voltage profiles were observed for a day to observe the depletion of the substrate and OCV in MFC system without resistance. The system was fed with 650 mg/l COD and COD removal was observed for 10 hours after feeding. As seen from the graph, the COD removal efficiency was approximately 78% for the MFC reactor with biomass. The system was operated with an OCV of 0.72 V.

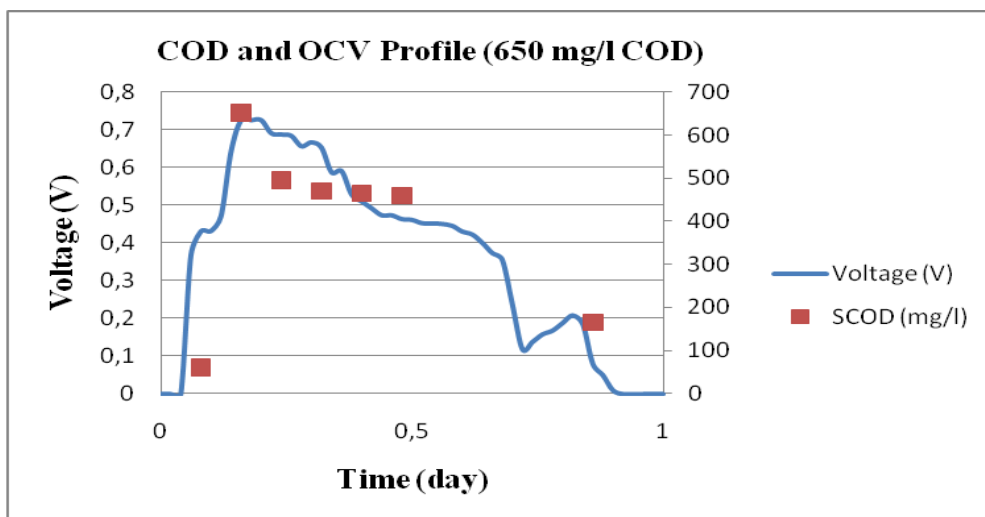


Figure 4.25: COD and OCV profile in the MFC fed with 650 mg/l COD without resistance.

4.2.4 MFC results for 650 mg/l COD concentration with external resistance

4.2.4.1 COD profiles

As seen from Figure 4.26, soluble influent and effluent COD profiles were observed for 6 days in the MFC system with 1 kΩ resistance. The system was fed with 650 mg/l COD and the COD removal efficiency was approximately 76% for the MFC reactor with external resistance.

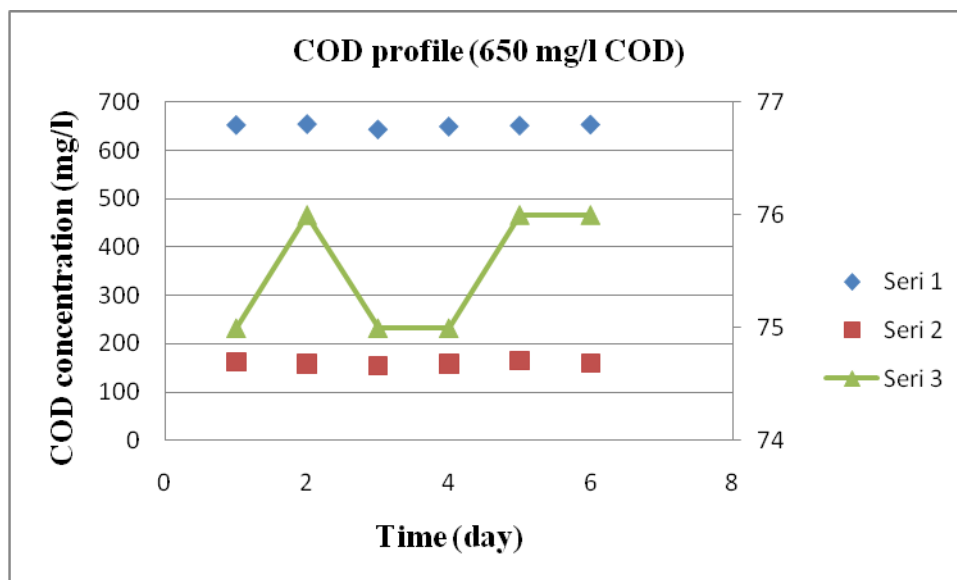


Figure 4.26: Influent and effluent COD concentrations and COD removal efficiencies in the MFC reactor fed with 650 mg/l COD.

COD removal monitored during 4 hours after feeding shows that (Figure 4.27), the substrate was depleted in MFC system with 1 kΩ resistance, similar to the MFC with

no external resistance for 6 days. As seen from the graph, more than 25% of the of COD was removed after 1 hour feeding.

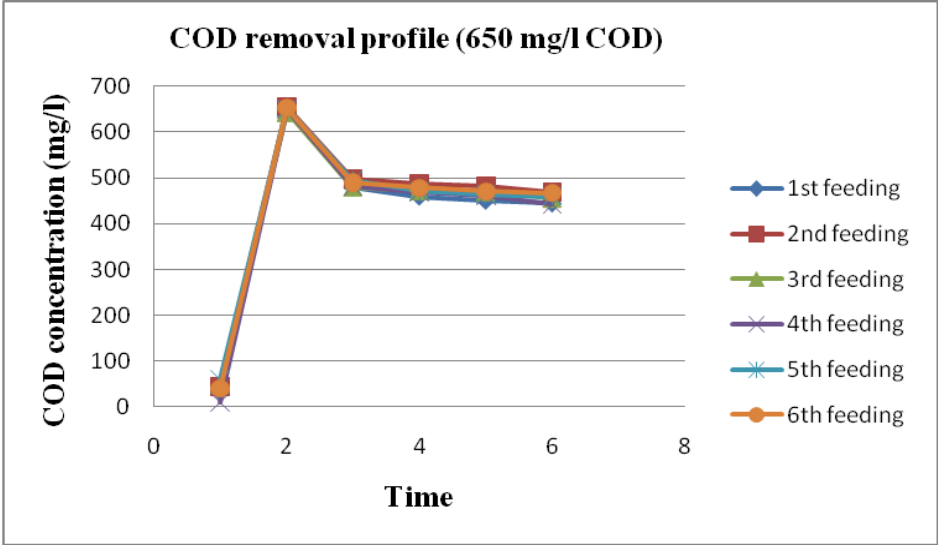


Figure 4.27: COD removal in the MFC reactor fed with 650 mg/l COD.

4.2.4.2 MLSS and MLVSS profiles

The mixed liquor MLVSS concentration was kept at 1500 mg/L (Figure 4.28). The daily MLVSS concentrations were monitored and the amount of excess sludge produced was determined as 200 ml/day. During this period, the amount of excess sludge was approximately constant and the system is said to be operated at steady-state with sludge age of 13 days.

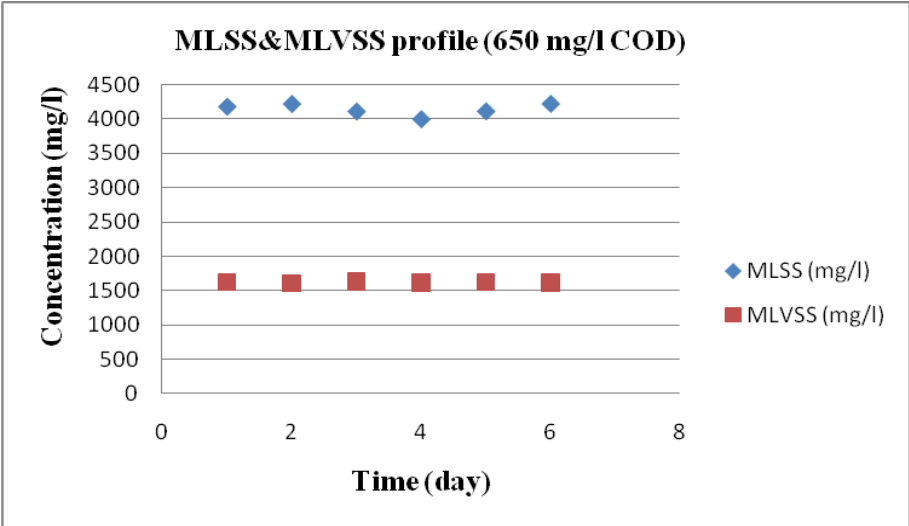


Figure 4.28: MLSS-MLVSS concentrations in the MFC reactor fed with 650 mg/l COD.

4.2.4.3 pH profile

As seen from Figure 4.29, the pH in the anodic chamber of MFC system was approximately between 7.0-7.2. The daily pH was measured and the system is said to be operated at neutral pH.

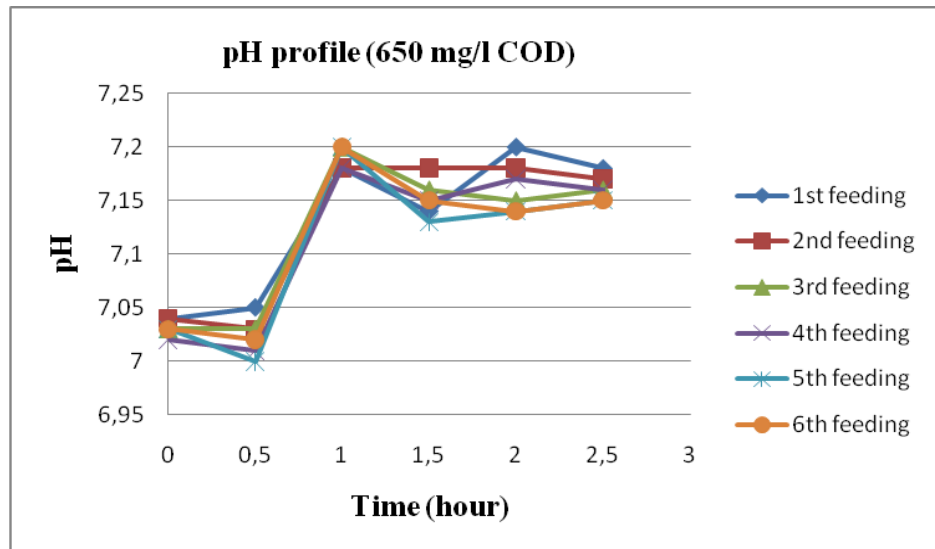


Figure 4.29: pH profiles in the MFC reactor fed with 650 mg/l COD.

4.2.4.4 Voltage profile with suspended biomass and 1 kΩ resistance

As seen from Figure 4.30, the electricity generation in the system fed with 650 mg/l COD, having 1500 mg/l suspended biomass and equipped with 1kΩ resistance was stable, exerting daily average maximums of 0.47 V at beginning of cycle.

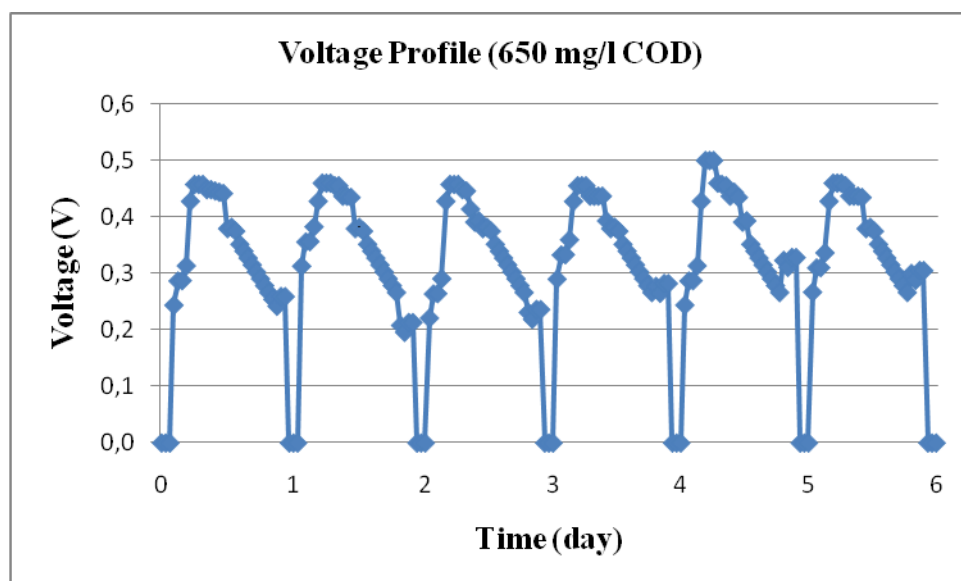


Figure 4.30: Voltage profile in the MFC fed with 650 mg/l COD.

4.2.4.5 Power and current profile

The current and power were calculated as given in the Materials and Methods section. As seen from Figure 4.31, the current and power profiles were obtained for 6 days. The average current and power were 0.47 mA and 217 mW, respectively.

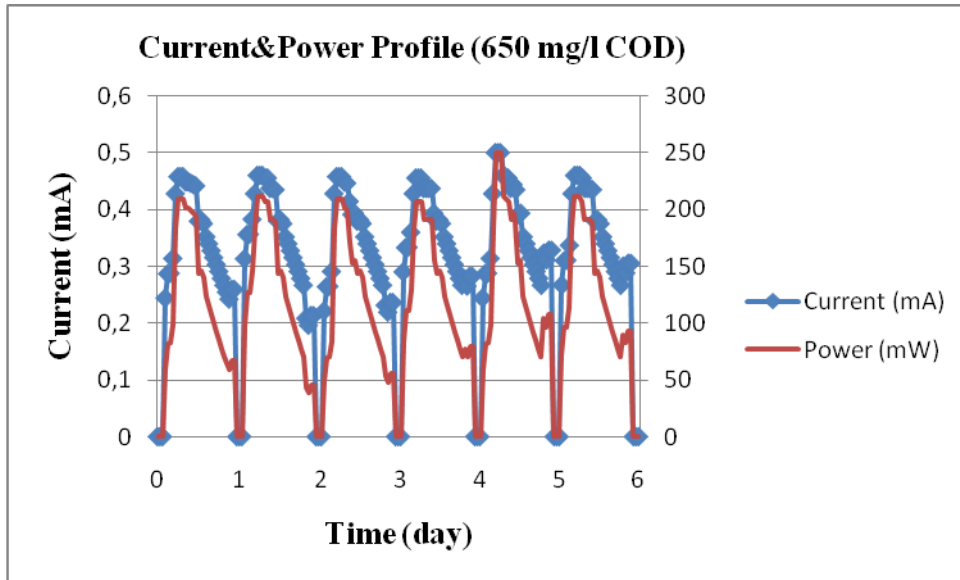


Figure 4.31: Current and power profiles in MFC fed with 650 mg/l COD.

4.2.4.6 Density profiles

The current and power densities were calculated as given in the Materials and Methods section. As seen from Figure 4.32, the current and power profiles were obtained for 6 days. The average current and power densities obtained during each cycle were 22.2 mA.m⁻² and 11111 mW.m⁻², respectively.

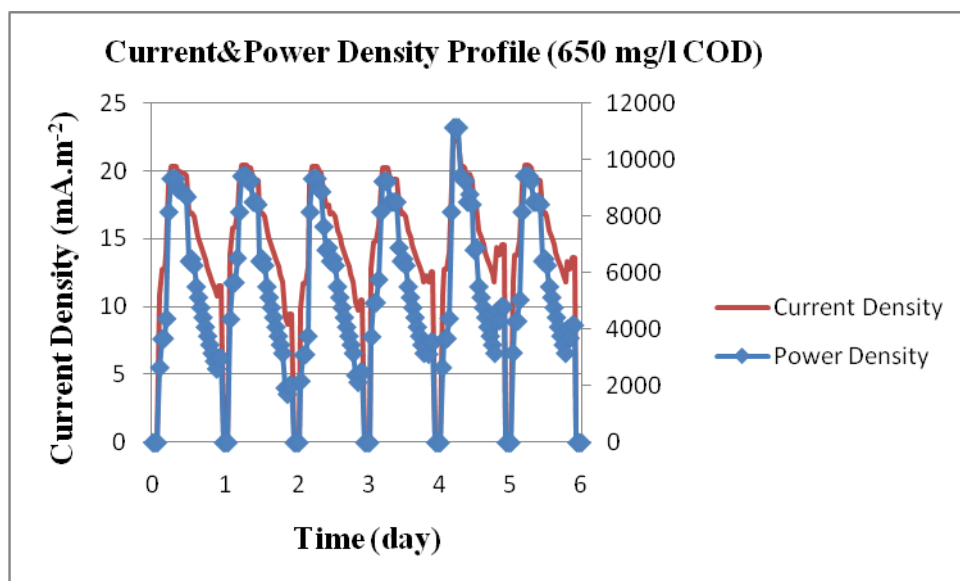


Figure 4.32: Current and power density profiles in MFC fed with 650 mg/l COD.

4.2.4.7 Polarization curve experiment result for 650 mg/l COD

The polarization curve was obtained by plotting voltage versus current density with 5 different resistances ranging from $1\text{k}\Omega$ to $5\text{k}\Omega$ for 650 mg/l COD feeding. As seen from Figure 4.33, when voltage increases, the current density decreases. Internal resistance of the system was calculated from the slope of the curve.

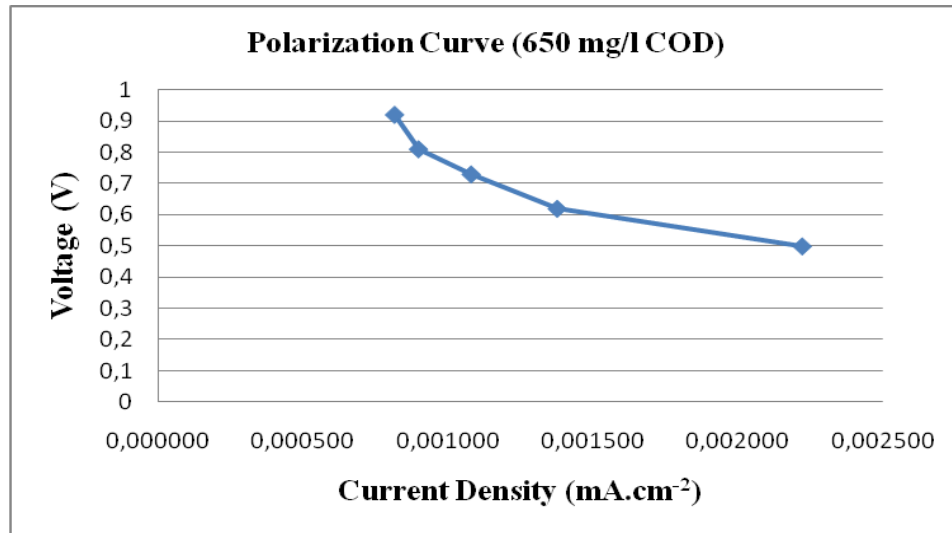


Figure 4.33: Polarization curve in the MFC fed with 650 mg/l COD.

4.2.5 MFC results for 160 mg/l COD concentration without external resistance

4.2.5.1 Voltage and COD profile

As seen from Figure 4.34, COD and voltage profiles were observed for a day to monitor the depletion of the substrate and OCV in MFC system without resistance. The system was fed with 160 mg/l COD and COD removal was observed for 10 hours after feeding. As seen from the graph, the COD removal efficiency was approximately 77% for a MFC reactor with biomass. MFC system with biomass is said to be operated with an OCV of 0.16 V.

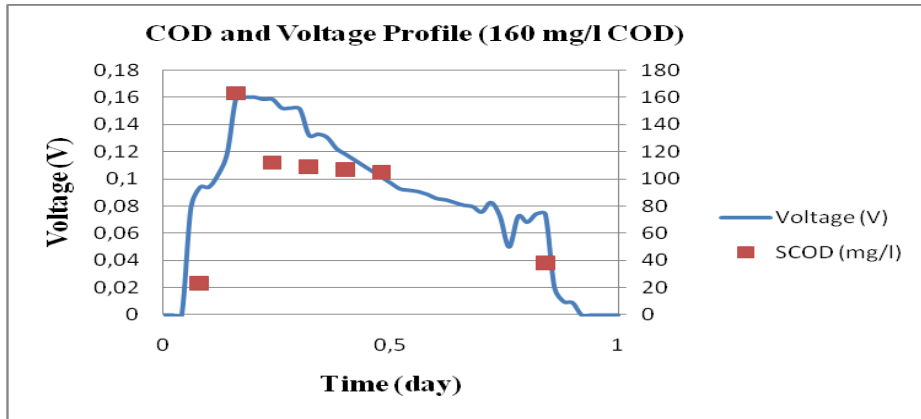


Figure 4.34: COD and OCV profile in the MFC fed with 160 mg/l COD without resistance.

4.2.6 MFC results for 160 mg/l COD concentration with external resistance

4.2.6.1 COD profiles

As seen from Figure 4.35, soluble influent and effluent COD profiles were observed for a 6 days in MFC system with 1 k Ω resistance. The system was fed with 160 mg/l COD and COD removal efficiency was approximately 77% for a MFC reactor with external resistance.

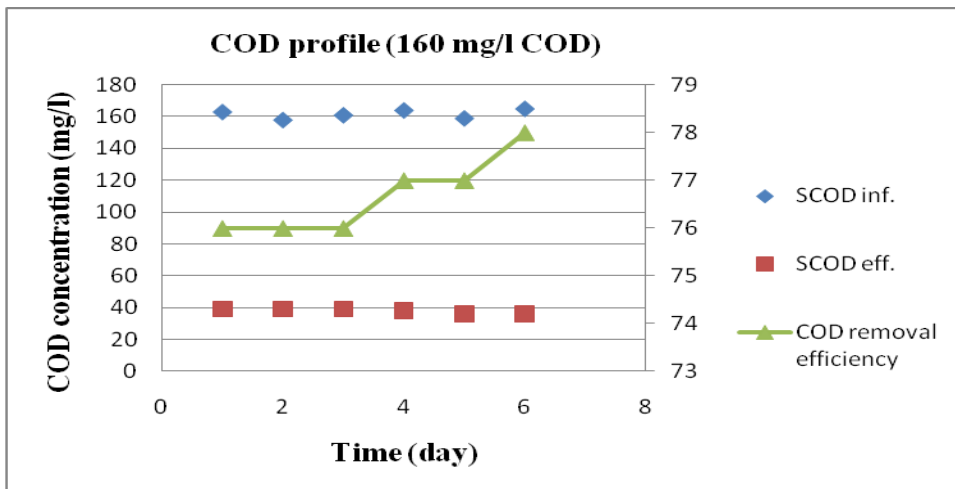


Figure 4.35: Influent and effluent COD concentrations and COD removal efficiencies in the MFC reactor fed with 160 mg/l COD.

COD removal of the monitored during 4 hours after feeding shows that (Figure 4.36), the substrate was depleted in MFC system with 1 k Ω resistance, similar to the MFC with no external resistance. As seen from the graph, more than 20% of the COD was removed 4 hours after feeding.

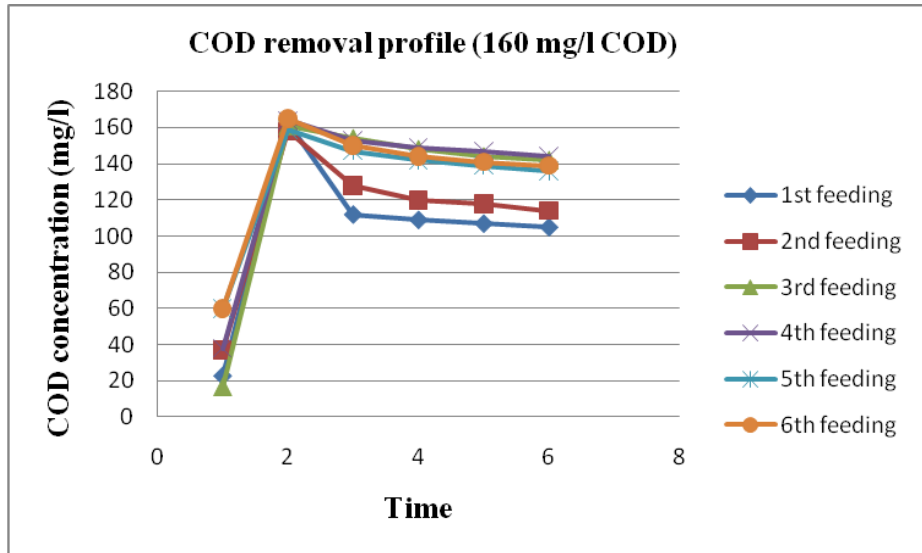


Figure 4.36: COD removal in the MFC reactor fed with 160 mg/l COD.

4.2.6.2 MLSS and MLVSS profiles

The mixed liquor MLVSS concentration was kept at 1500 mg/L (Figure 4.37). The daily MLVSS concentrations were monitored and the amount of excess sludge produced was determined as 80 ml/day. During this period, the amount of excess sludge was approximately constant and the system is said to be operated at steady-state with sludge age of 31 days.

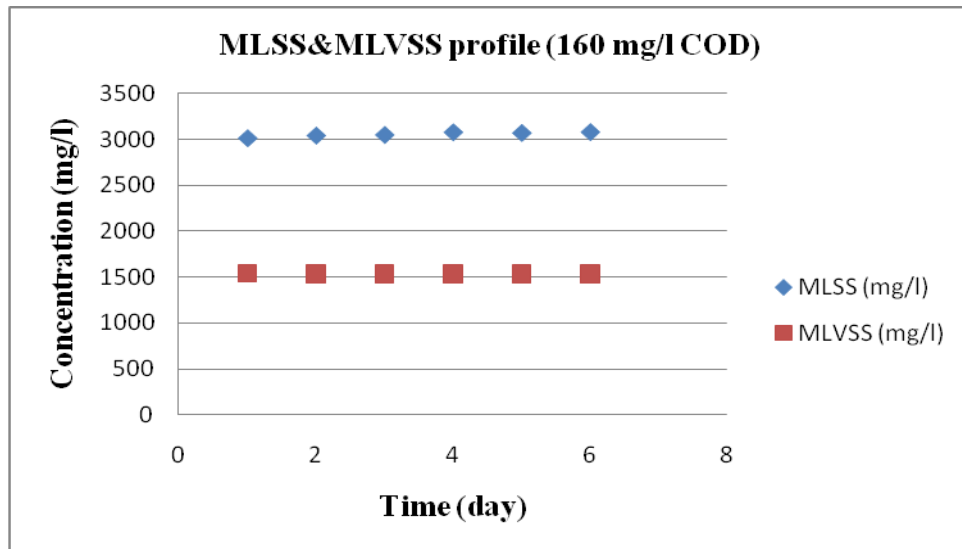


Figure 4.37: MLSS-MLVSS concentrations in the MFC reactor fed with 160 mg/l COD

4.2.6.3 pH profile

As seen from Figure 4.38, the pH in the anodic chamber of MFC system was approximately between 7.0-7.2. The daily pH was measured and the system is said to be operated at neutral pH.

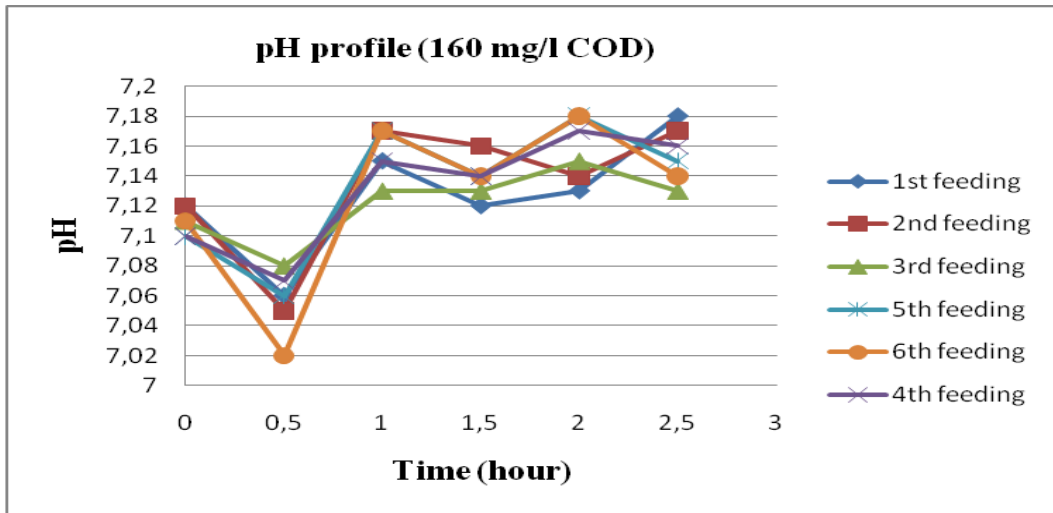


Figure 4.38: pH profiles in the MFC reactor fed with 160 mg/l COD.

4.2.6.4 Voltage profile with suspended biomass and 1 kΩ resistance

As seen from Figure 4.39, the electricity generation in MFC system with 1500 mg/l biomass and 1 kΩ external resistance was 0.13 V on the average for 6 days of operation. The voltage profiles were similar for each cycle.

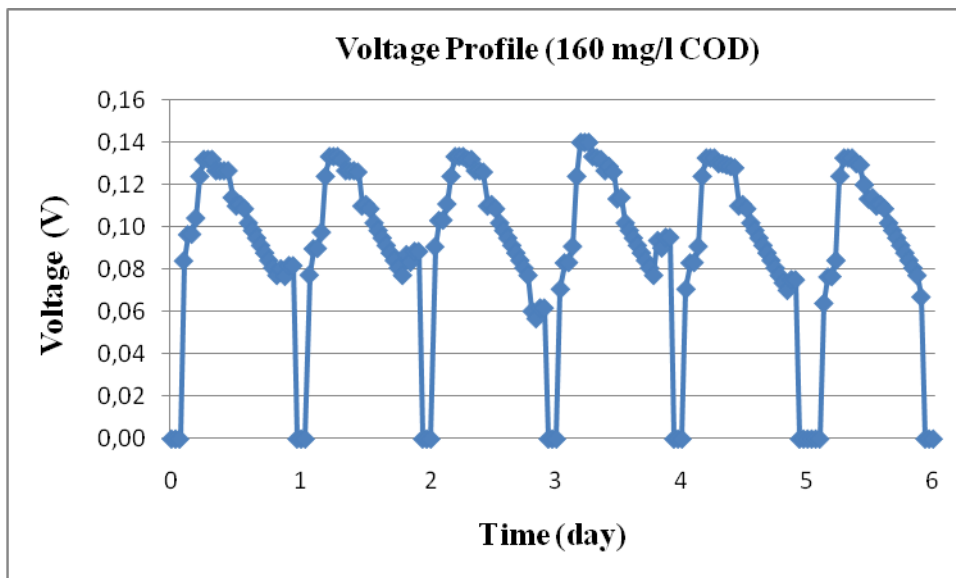


Figure 4.39: Voltage profile in the MFC fed with 160 mg/l COD.

4.2.6.5 Power and current profile

The current and power were calculated as given in the Materials and Methods section. As seen from Figure 4.40, the current and power profiles were obtained for 6 days. The average current and power were 0.13 mA and 18 mW, respectively.

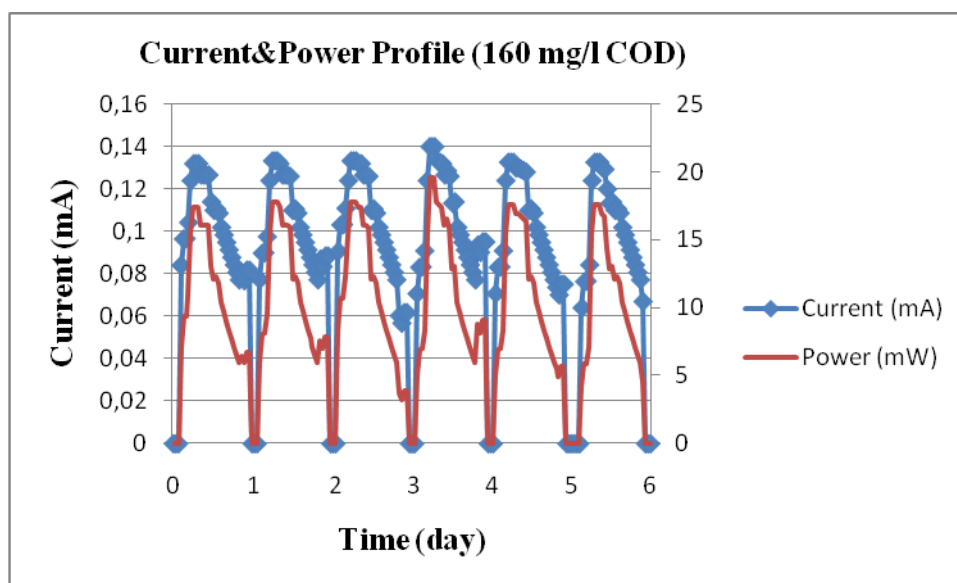


Figure 4.40: Current and power profiles in MFC fed with 160 mg/l COD.

4.2.6.6 Density profiles

The current and power densities were calculated as given in the Materials and Methods section. As seen from Figure 4.41, the current and power profiles were obtained for 6 days. The average current and power densities obtained during each cycle were 5.9 mA.m⁻² and 871 mW.m⁻², respectively.

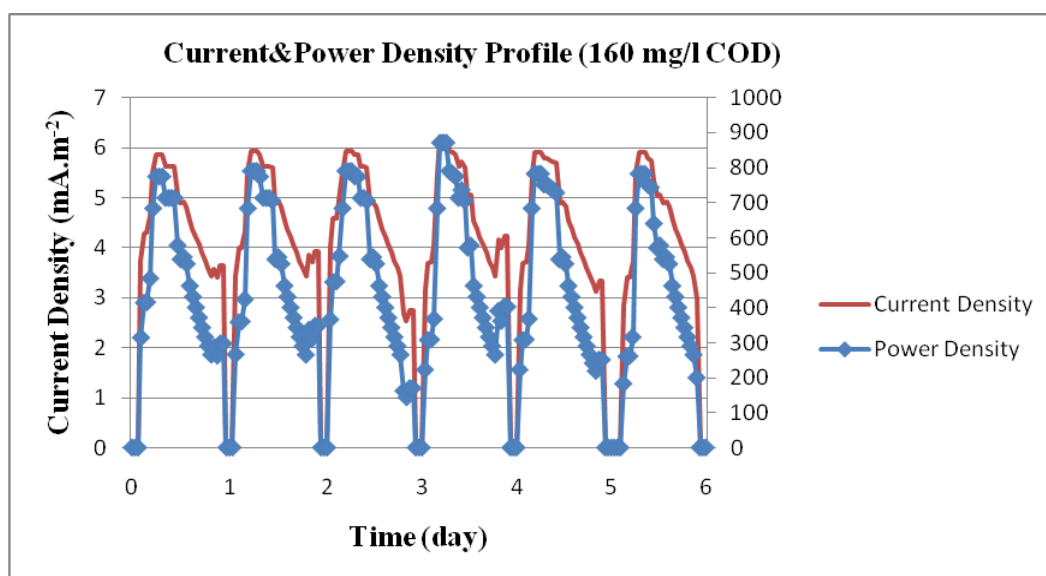


Figure 4.41: Current and power density profiles in MFC fed with 160 mg/l COD.

4.2.6.7 Polarization curve experiment result for 160 mg/l

The polarization curve was obtained by plotting voltage versus current density with 5 different resistance ranging from 1 k Ω to 5 k Ω for 160 mg/l COD feeding. As seen from Figure 4.42, when voltage increases, the current density decreases. Internal resistance of the system was calculated from the slope of the curve.

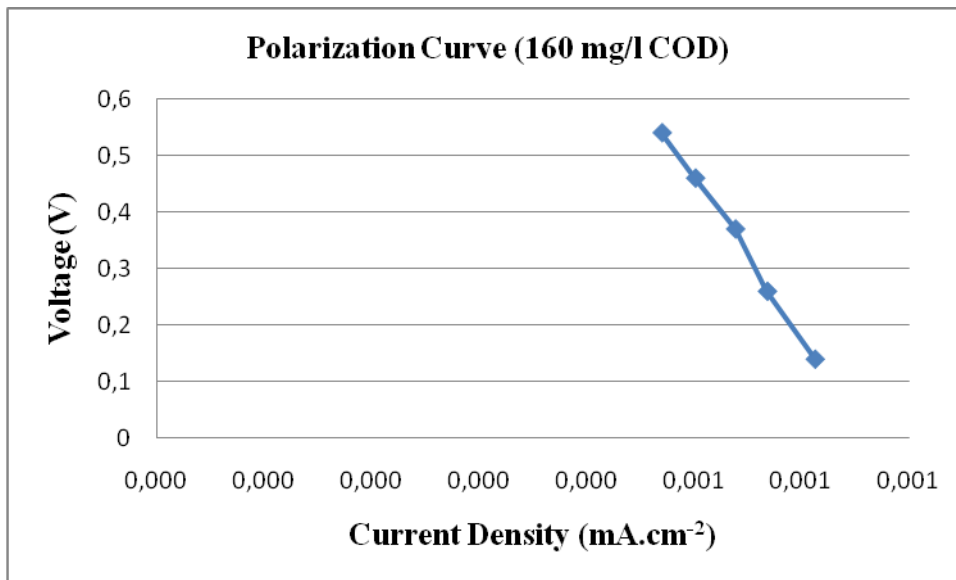


Figure 4.42: Polarization curve in the MFC fed with 160 mg/l COD.

5. RESULT AND DISCUSSION

This study was conducted to observe the performance of a two compartment MFC fed with synthetic wastewater prepared with sodium acetate as the carbon source. The work is focused on the study of the effect of the biodegradability of sodium acetate, paying special attention to the study of the relationship between COD removal and electricity generation, including the achievement of high power and current densities, in the MFC system with anodic and cathodic compartment volumes of 2.5 L. The anodic chamber was seeded with 1500 mgVSS/L biomass to simulate the conventional activated sludge systems. The cathodic chamber was filled with tap water and was continuously aerated. A two-compartment MFC with the anodic and the cathodic chambers separated by a proton exchange membrane was designed. The voltage generation was monitored with a multimeter connected to a computer for continuous data collection.

Experimental results showed that the two-compartment MFC could generate electricity using sodium acetate as substrate, and the required electrically active bacteria presented in the wastewater. When synthetic wastewater was introduced into MFC, an initial circuit voltage of 0.037 V was immediately generated which might be due to the difference of the potential between the two electrodes based on both chemical and biological factors. Thereafter, the voltage increased because of biological activity, and stabilized at about 0.201 V in 15 days after start-up period.

Carbon removal and electricity generation efficiencies were observed for different feeding conditions where 160 mg COD/l, 325 mg COD/l, and 650 mg COD/l was fed to the system. Each set of experiments were run for 1 week and daily cycles of fill and draw operation was applied. The system was monitored for pH and MLVSS changes and COD removal by the collection of the samples at predetermined intervals. Figure 5.1 presents the OCV profiles of MFC system for each substrate concentration. As shown in the Figure 5.1, electricity generation of each concentration included three phases: ascending phase, stationary phase and declining phase. Apparently, data showed higher voltage outputs for 650 mg/l COD (0.72 V) than those for 325 (0.3 V) and 160 mg/l COD (0.16 V).

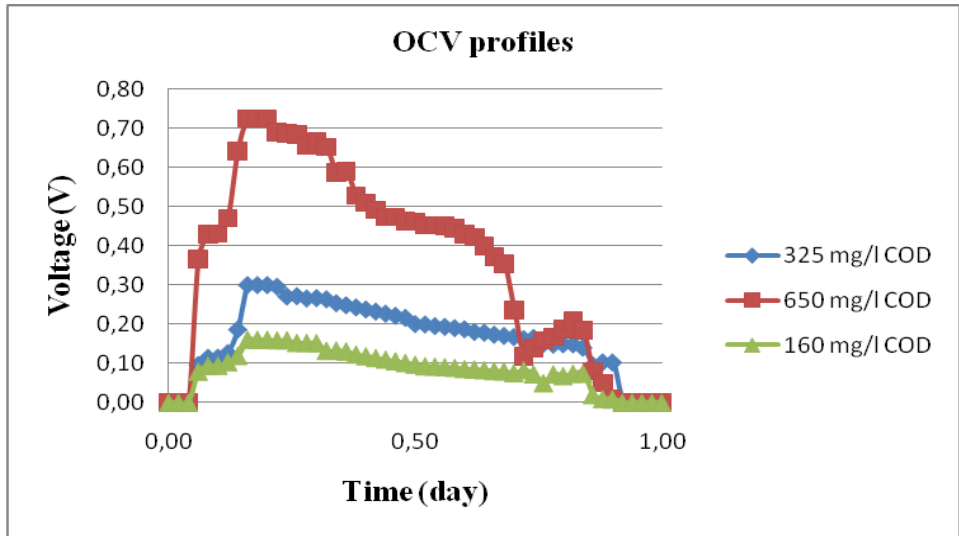


Figure 5.1: OCV profile for each substrate concentration.

After determination of OCV a 1000Ω external resistance was connected to the MFCs which were fed with a sodium acetate with a different COD concentration of 160 mg/l COD, 325 mg/l COD and 650 mg/l COD. As seen from the voltage profiles the period of ascending phases in the first cycle lasted longer than the following cycles, likely caused by the enriching and forming processes of electrically active bacteria biofilms on the anode electrode. Data showed higher voltage outputs in the latter cycles than those in the first one. As shown in the Figure 5.2, the maximum voltage was increased with the increasing feed concentrations.

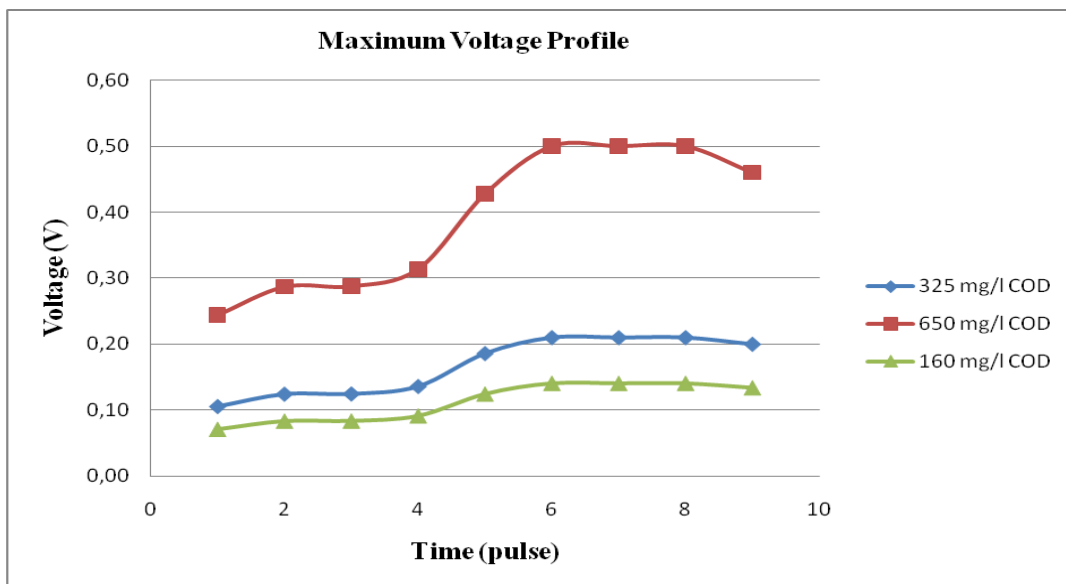


Figure 5.2: Maximum voltage profiles for each substrate concentration.

In a fill and draw cycle, once MFC stabilized at the maximum steady voltage, the polarization curve was obtained by recording the voltage via varying the external

resistance from 1000Ω to 5000Ω . The maximum power density and current density were calculated from the formula as mentioned in previous sections. Figure 5.3 shows that power density increased with the feeding concentration and the maximum power density increased from 80 to 963 mW/m^2 .

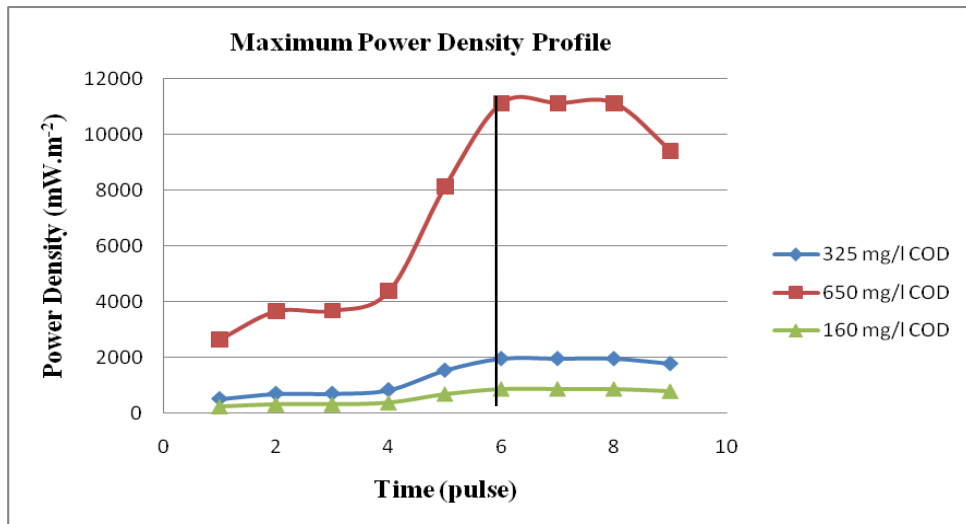


Figure 5.3: Maximum power density profile for each substrate concentration.

A similar trend was observed in the current density as seen in Figure 5.4. This trend in the power and current densities might be due to the change of the internal resistance.

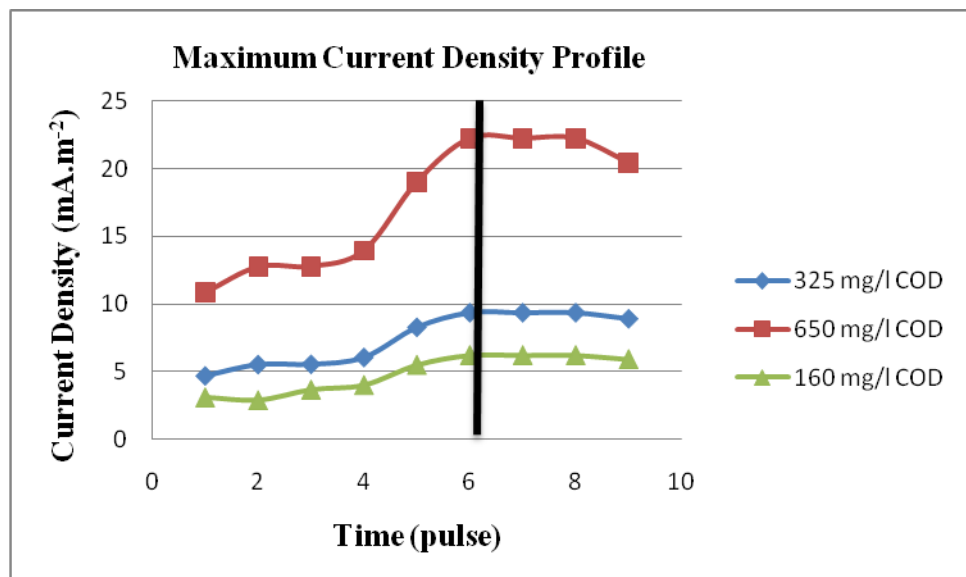


Figure 5.4: Maximum current density profile for each substrate concentration.

Over the whole experimental period, the maximum power density of 80, 180 and 963 mW/m^2 occurred at 1000Ω with a current density of 0.6, 0.9 and 2.07 mA/m^2 for 160 and 320 and 650 mg/l COD, respectively.

According to Ohm's law, the internal and external resistances are equal in the case that the power density is maximum. Figure 5.5. shows a curve of voltage as a function of current was established by varying external resistance, and the slopes of plots represented internal resistances of MFCs, consistent with the values obtained from polarization curve. It is evident from the experimental data that the voltage–current density curve can be roughly divided into three stages: activation polarization, ohmic loss and concentration polarization. At the first stage, current was relatively low, activation resistance caused by reaction kinetics played a dominant role, which caused a rapid voltage decrease. As current increased, polarization curve showed a linear relationship between voltage and current, which is called ohmic polarization, resulted from ionic resistance and electronic resistance. In this phase, there was also non-ohmic polarization; when external resistance was equal to internal resistance (1000Ω), power density reached the maximum of 87, 196 and 1111 mW/m^2 . With continued increase of current density, the effect of substrate concentration became obvious.

As shown in Fig. 5.6, the internal resistance decreased when COD concentration increased which was an opposite trend to power density. The change of internal resistance is related to bacterial activity. A decrease in internal resistance might be a consequence of increased microbial activity, resulted from enrichment and maturation of the biofilm on the anode, and the following increase might be a consequence of decreased activity, due to the biofilm aging and abscission.

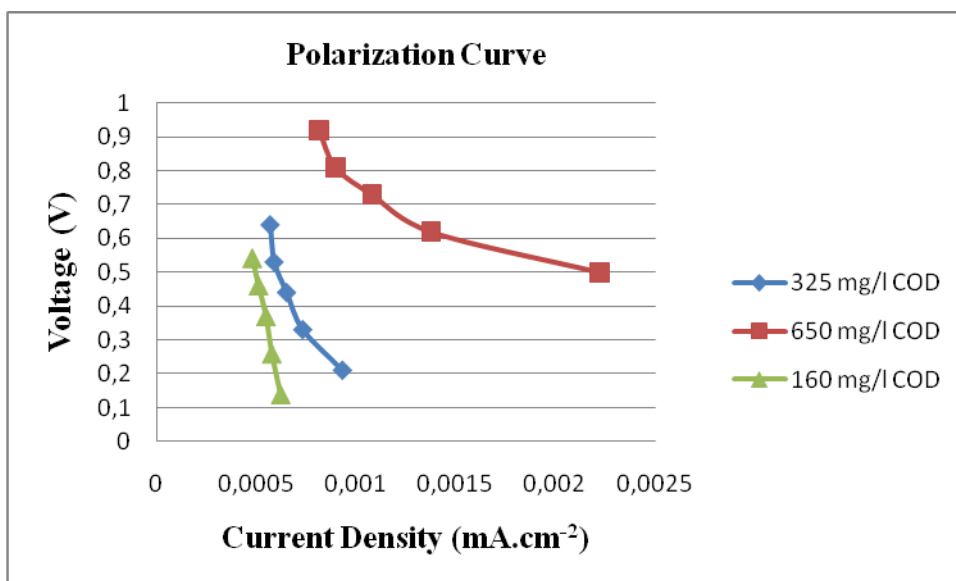


Figure 5.5: Polarization curves of MFC system for different COD concentrations.

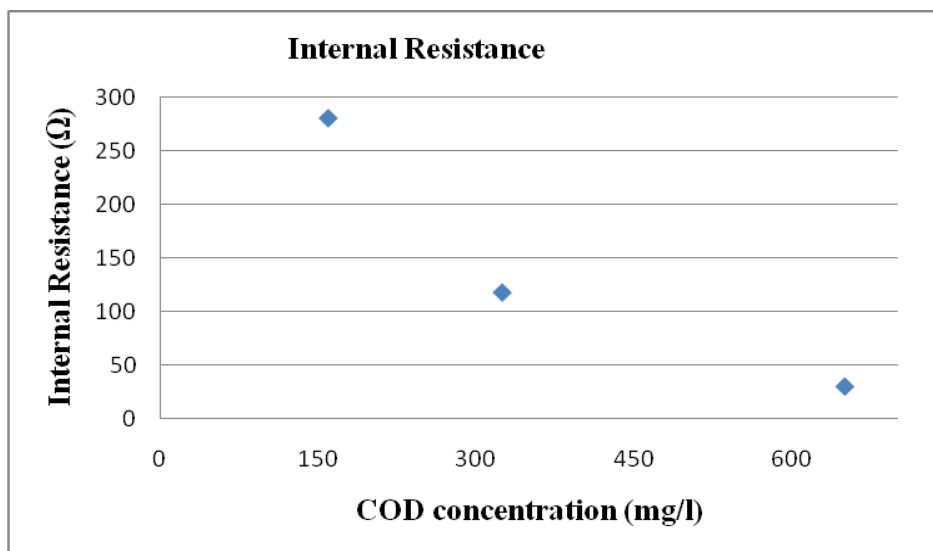


Figure 5.6: Internal resistance of MFC system for different COD concentrations.

MFC used for wastewater treatment, which resembles anaerobic suspended growth contact reactor, documented its capacity in treating wastewater in association with power generation. Figure 5.7 shows the results of efficiency of wastewater degradation. In the experiment, the hydraulic residence time was kept at 24 h and influent COD was controlled between 160 and 650 mg/L. Data showed that as voltage generation increased, effluent COD amount decreased, but only slightly, from 39 to 36 mg/L for 160 mg/l COD, and from 73 to 71 mg/L for 325 mg/l COD and from 158 to 155 mg/L for 650 mg/l COD. COD removal efficiencies remained 77%, 78% and 76% for 160, 320 and 650 mg/l COD, respectively. This result indicated that the reactor has a well stability in wastewater treatment in various conditions.

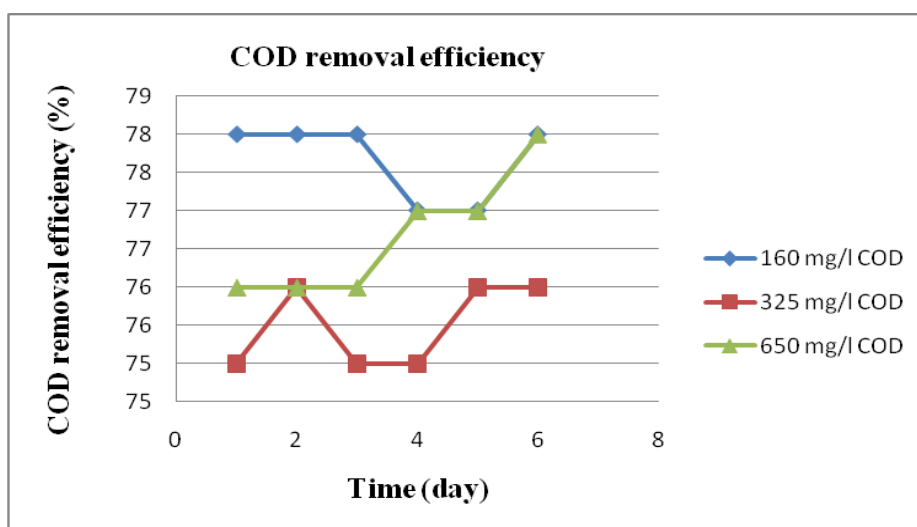


Figure 5.7: COD removal efficiency profile for each substrate concentration.

Coulombic efficiency (CE) is shown in Figure 5.8. As current density increased, CE increased linearly. According to formula data as mentioned above, it can be seen that ΔCOD is nearly independent of R, thus the theoretical electricity production had a little change. However, as current increased, total electrons obtained in the experiment increased, which resulted in an increasing CE.

A maximum CE of 0.7% was obtained at external resistance of 1000 Ω , which is quite lower than CE of synthetic wastewater of (Liu and Logan, 2004). There are many possible reasons for such a low Coulombic efficiency, such as oxygen diffusion to the wastewater, etc.

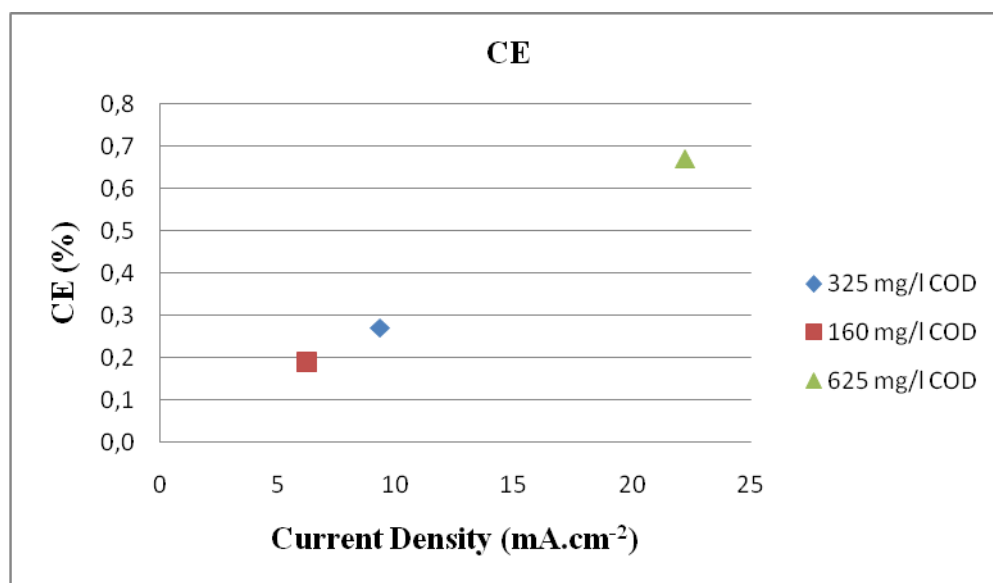


Figure 5.8: CE profile for each substrate concentration.

The experimental studies performed in this Thesis showed that a large volume two compartment MFC could be used to generate electricity coupled with efficient COD removal. The designed and constructed MFC system equipped with relatively cheap electrodes (stainless steel plates) could be operated at similar current and power densities reported in the literature. Experiments with different feed concentrations showed that the MFC system could produce higher electricity outputs per unit amount of organic matter at higher substrate concentrations with the same COD removal efficiencies. The studies presented in this work present the applicability of MFC concept into conventional suspended growth activated sludge systems. Thus, the study can be regarded as an initiation for upgrading the conventional activated sludge systems to generate electrical power using stable and inexpensive materials as electrodes, which will add to the feasibility of MFC applications.

The overview of the experimental results obtained for three sets of experiments are given in Table 5.1.

Table 5.1: Overview of the experimental results for the MFC system under different feeding conditions.

Feeding concentration \rightarrow	160 mg/l COD	325 mg/l COD	650 mg/l COD
Parameters \downarrow			
MLVSS concentration (mg/l)	1500	1500	1500
F/M ratio (gCOD/gVSS)	0.11	0.22	0.43
Hydraulic Retention Time (day)	2	2	2
Sludge Retention Time (Sludge Age, day)	32	20	13
COD removal (%)	77	78	76
pH	7.00-7.20	7.00-7.15	7.00-7.20
OCV (V)	0.16	0.3	0.72
Maximum Voltage with 1 kΩ resistance (V)	0.13	0.2	0.47
Maximum Current (mA)	0.13	0.2	0.47
Maximum Power(mW)	18	40	217
Maximum Current density (mA.m⁻²)	5.9	9.33	22.2
Maximum power density (mW.m⁻²)	871	1960	11111
Internal Resistance (mΩ)	281	118	30
Coulombic efficiency (%)	0.19	0.27	0.67

REFERENCES

- Aelterman, P., Rabaey, K., Pham, HT., Boon, N. and Verstraete W.,** 2006. Continuous electricity generation at high voltages and currents using stacked microbial fuel cells. *Environ Sci Tech.*, **40**, 3388–3394.
- Allen, RM. and Bennetto, HP.,** 1993. Microbial fuel-cells: electricity production from carbohydrates. *Appl Biochem Biotechnol.*, **39/40**, 27–40.
- Appleby, AJ. and Fouldes FR.,** 1989. Fuel cell handbook. New York: Van Nostrand Reinhold.
- Bennetto, HP.,** 1984. Microbial fuel cells. *Life Chem Rep* **2**, 363–453.
- Bergel, A., Feron, D. and Mollica, A.,** 2005. Catalysis of oxygen reduction in PEMfuel cell by seawater biofilm. *Electrochem Commun.*, **7**, 900–904.
- Bond, DR. and Lovley, DR.,** 2003. Electricity production by *Geobacter sulfurreducens* attached to electrodes. *Appl Environ Microbiol.*, **69**, 1548–1555.
- Bullen, RA., Arnot, TC., Lakeman, JB. and Walsh FC.,** 2006. Biofuel cells and their development. *Biosens Bioelectron.*, **21**, 2015–45.
- Chang, IS., Jang, JK., Gil, GC., Kim, M., Kim, HJ. and Cho, BW.,** 2004. Continuous determination of biochemical oxygen demand using microbial fuel cell type biosensor. *Biosens Bioelectron.*, **19**, 607–613.
- Chang, IS., Moon, H., Jang, JK. and Kim BH.,** 2005. Improvement of a microbial fuel cell performance as a BOD sensor using respiratory inhibitors. *Biosens Bioelectron.*, **20**, 1856–1859.
- Chang, IS., Moon, H., Bretschger, O., Jang, JK., Park, HI. and Nealson, KH.,** 2006. Electrochemically active bacteria (EAB) and mediator-less Microbial fuel cells. *J Microbiol Biotechnol.*, **16**, 163–177.
- Chaudhuri, SK. and Lovley, DR.,** 2003. Electricity generation by direct oxidation of glucose in mediatorless microbial fuel cells. *Nat Biotechnol.*, **21**, 1229–1232.
- Cheng, S., Liu, H. and Logan BE.,** 2006a. Increased performance of single-chamber microbial fuel cells using an improved cathode structure. *Electrochem Commun.*, **8**, 489–494.
- Cheng, S., Liu, H. and Logan BE.,** 2006b. Increased power generation in a continuous flow MFC with advective flow through the porous anode and reduced electrode spacing. *Environ Sci Technol.*, **40**, 2426–2432.
- Cheng, S., Liu, H. and Logan, BE.,** 2006c. Power densities using different cathode catalyst (Pt and CoTMPP) and polymer binders (Nafion and PTFE) in single chamber microbial fuel cells. *Environ Sci Technol.*, **40**, 364–369.

- Chia, M.A.**, 2002. Technical digest of solid state sensors and actuators workshop, *HiltonHead Island.*, 59–60.
- Choi, Y., Jung, E., Kim, S. and Jung S.**, 2003. Membrane fluidity sensing microbial fuel cell. *Bioelectrochemistry.*, **59**, 121–127.
- Davis, F. and Higson, SPJ.**, 2007. Biofuel cells—recent advances and applications. *Biosens Bioelectron.*, **22**, 1224–1235.
- Delong, EF. and Chandler, P.**, 2002. Power from the deep. *Nat Biotechnol.*, **20**, 788–789.
- Gil, GC., Chang, IS., Kim, BH., Kim, M., Jang, JY. and Park, HS.**, 2003. Operational parameters affecting the performance of a mediatorless microbial fuel cell. *Biosens Bioelectron.*, **18**, 327–334.
- Gregory, KB., Bond, DR. and Lovley, DR.**, 2004. Graphite electrodes as electron donors for anaerobic respiration. *EnvironMicrobiol.*, **6**, 596–604.
- Habermann, W. and Pommer, EH.**, 1991. Biological fuel cells with sulphide storage capacity. *Appl Microbiol Biotechnol.*, **35**, 128–133.
- He, Z., Minteer, SD. and Angenent L.**, 2005. Electricity generation from artificial wastewater using an upflow microbial fuel cell. *Environ Sci Technol.*, **39**, 5262–5267.
- He, Z, Wagner, N., Minteer, SD. and Angenent LT.**, 2006. An upflow microbial fuel cell with an interior cathode: assessment of the internal resistance by impedance spectroscopy. *Environ Sci Technol.*, **40**, 5212–5217.
- Hernandez, ME. and Newman, DK.**, 2001. Extracellular electron transfer. *Cell Mol Life Sci.*, **58**, 1562–1571.
- Holzman, DC.**, 2005. Microbe power. *Environ Health Persp.*, **113** (A), 754–757.
- Ieropoulos, I., Greenman, J. and Melhuish, C.**, 2003a. Imitation metabolism: energy autonomy in biologically inspired robots. *Proceedings of the 2nd international symposium on imitation of animals and artifacts.*, 191–194.
- Ieropolulos, I., Melhuish, C. and Greenman, J.**, 2003b. Artificial metabolism: towards true energetic autonomy in artificial life. *Lect Notes Comput Sc.*, **2801**, 792–799.
- Ieropoulos, I., Melhuish, C. and Greenman, J.**, 2004. Energetically autonomous robots. In: Groen F, et al, editor. *Intelligent autonomous systems.*, vol. **8**. Amsterdam: IOS Press., 128–135.
- Ieropoulos, IA., Greenman, J., Melhuish, C. and Hart, J.**, 2005a. Comparative study of three types of microbial fuel cell. *Enzyme Microb Tech.*, **37**, 238–245.
- Ieropoulos, I., Melhuish, C. and Greenman, J.**, 2005c. EcoBot-II: an artificial agent with a natural metabolism. *Adv Robot Syst.*, **2**, 295–300.
- Jang, JK., Pham, TH., Chang, IS., Kang, KH., Moon, H. and Cho, KS.**, 2004. Construction and operation of a novel mediator-and membraneless microbial fuel cell. *Process Biochem.*, **39**, 1007–1012.

- Kang, KH., Jang, JK., Pham, TH., Moon, H., Chang, IS. and Kim, BH.,** 2003. A microbial fuel cell with improved cathode reaction as a low biochemical oxygen demand sensor. *Biotechnol Lett.*, **25**, 1357–1361.
- Kim, BH., Kim, HJ., Hyun, MS. and Park DH.,** 1999a. Direct electrode reaction of Fe (III)-reducing bacterium, *Shewanella putrifaciens*. *J Microbiol Biotechnol.*, **9**, 127–131.
- Kim, HJ., Park, HS., Hyun, MS., Chang, IS., Kim, M. and Kim BH.,** 2002. A mediatorless microbial fuel cell using a metal reducing bacterium, *Shewanella putrefaciens*. *Enzyme Microb Tech.*, **30**, 145–152.
- Kim, BH., Chang, IS., Gil, GC., Park, HS. and Kim HJ.,** 2003. Novel BOD (biological oxygen demand) sensor using mediator-less microbial fuel cell. *Biotechnol Lett.*, **25**, 541–545.
- Kim, BH., Park, HS., Kim, HJ., Kim, GT., Chang, IS. and Lee, J.,** 2004. Enrichment of microbial community generating electricity using a fuel-cell type electrochemical cell. *Appl Microbiol Biotechnol.*, **63**, 672–681.
- Kim, JR., Min, B. and Logan BE.,** 2005. Evaluation of procedures to acclimate a microbial fuel cell for electricity production. *Appl Microbiol Biotechnol.*, **68**, 23–30.
- Liu, H. and Logan, BE.,** 2004. Electricity generation using an air-cathode single chamber microbial fuel cell in the presence and absence of a proton exchange membrane. *Environ Sci Technol.*, **38**, 4040–4046.
- Liu, H., Ramnarayanan, R. and Logan, BE.,** 2004. Production of electricity during wastewater treatment using a single chamber microbial fuel cell. *Environ Sci Technol.*, **28**, 2281–2285.
- Liu, H., Cheng, S. and Logan, BE.,** 2005a. Production of electricity from acetate or butyrate using a single-chamber microbial fuel cell. *Environ Sci Technol.*, **39**, 658–662.
- Liu, H., Cheng, S. and Logan, BE.,** 2005b. Power generation in fed-batch microbial fuel cells as a function of ionic strength, temperature, and reactor configuration. *Environ Sci Technol.*, **39**, 5488–5493.
- Liu, H., Grot, S. and Logan, BE.,** 2005c. Electrochemically assisted microbial production of hydrogen from acetate. *Environ Sci Technol.*, 4317–4320.
- Logan, BE., Hamelers, B., Rozendal, R., Schroder, U., Keller, J. and Freguia, S.,** 2006. Microbial fuel cells: methodology and technology. *Environ Sci Technol.*, **40**, 5181–5192.
- Lovley, DR.,** 1993. Dissimilatory metal reduction. *Annu Rev Microbiol.*, **47**, 263–290.
- Lovely, DR.,** 2006. Microbial fuel cells: novel microbial physiologies and engineering approaches. *Curr Opin Biotech.*, **17**, 327–332.
- Madigan, MT., Martinko, JM. and Parker J.,** 2000. Brock biology of microorganisms. Upper Saddle River: Prentice Hall.

- Melhuish, C., Ieropoulos, I., Greenman, J. and Horsfield, I.,** 2006. Energetically autonomous robots: food for thought. *AutonRobot.*, **21**, 187–198.
- Min, B. and Logan, BE.,** 2004. Continuous electricity generation from domestic wastewater and organic substrates in a flat plate microbial fuel cell. *Environ Sci Technol.*, **38**, 5809–5814.
- Min, B., Cheng, S. and Logan, BE.,** 2005a. Electricity generation using membrane and salt bridge microbial fuel cells. *Water Res.*, **39**, 1675–1686.
- Min, B., Kim, JR., Oh, SE., Regan, JM. and Logan BE.,** 2005b. Electricity generation from swine wastewater using microbial fuel cells. *Water Res.*, **39**, 4961–4968.
- Moon, H., Chang, IS., Kang, KH., Jang, JK. and Kim, BH.,** 2004. Improving the dynamic response of a mediator-less microbial fuel cell as a biochemical oxygen demand (BOD) sensor. *Biotechnol Lett.*, **26**, 1717–1721.
- Moon, H., Chang, IS., Jang, JK. and Kim BH.,** 2005. Residence time distribution in microbial fuel cell and its influence on COD removal with electricity generation. *Biochem Eng J.*, **27**, 59–65.
- Moon, H., Chang, IS. and Kim BH.,** 2006. Continuous electricity production from artificial wastewater using a mediator-less microbial fuel cell. *Bioresource Technol.*, **97**, 621–627.
- Oh, SE. and Logan, BE.,** 2005. Hydrogen and electricity production from a food processing wastewater using fermentation and microbial fuel cell technologies. *Water Res.*, **39**, 4673–4682.
- Oh, SE. and Logan, BE.,** 2006. Proton exchange membrane and electrode surface areas as factors that affect power generation in microbial fuel cells. *Appl Microbiol Biotechnol.*, **70**, 162–169.
- Oh, SE., Min, B. and Logan, BE.,** 2004. Cathode performance as a factor in electricity generation in microbial fuel cells. *Environ Sci Technol.*, **38**, 4900–4944.
- Park, DH. and Zeikus, JG.,** 1999. Utilization of electrically reduced neutral red by *Actinobacillus succinogenes*: physiological function of neutral red in membrane-driven fumarate reduction and energy conservation. *J Bacteriol.*, **181**, 2403–2410.
- Park, DH. and Zeikus, JG.,** 2000. Electricity generation in microbial fuel cells using neutral red as an electronophore. *Appl Environ Microb.*, **66**, 1292–1297.
- Park, DH. and Zeikus, JG.,** 2002. Impact of electrode composition on electricity generation in a single-compartment fuel cell using *Shewanella putrefaciens*. *Appl Microbiol Biotechnol.*, **59**, 58–61.
- Park, DH. and Zeikus, JG.,** 2003. Improved fuel cell and electrode designs for producing electricity from microbial degradation. *Biotechnol Bioeng.*, **81**, 348–355.
- Pham, TH., Jang, JK., Chang, IS. and Kim, BH.,** 2004. Improvement of cathode reaction of a mediatorless microbial fuel cell. *J Microbiol Biotechnol.*, **14**, 324–329.

- Pham, TH., Rabaey, K., Aelterman, P., Clauwaert, P., De Schampelaire, L., Boon, N. and Verstraete, W.,** 2006. Microbial fuel cells in relation to conventional anaerobic digestion technology. *Eng Life Sci.*, **6**, 285–292.
- Potter, MC.,** 1912. Electrical effects accompanying the decomposition of organic compounds. *Proc R Soc Ser B.*, **84**, 260–276.
- Prasad, D., Sivaram, TK., Berchmans, S. and Yegnaraman, V.,** 2006. Microbial fuel cell constructed with a micro-organism isolated from sugar industry effluent. *J Power Sources.*, **160**, 991–996.
- Rabaey, K. and Verstraete, W.,** 2005. Microbial fuel cells: novel biotechnology for energy generation. *Trends Biotechnol.*, **23**, 291–298.
- Rabaey, K., Lissens, G., Siciliano, S. and Verstraete, W.,** 2003. A microbial fuel cell capable of converting glucose to electricity at high rate and efficiency. *Biotechnol Lett.*, **25**, 1531–1535.
- Rabaey, K., Boon, N., Siciliano, SD., Verhaege, M. and Verstraete, W.,** 2004. Biofuel cells select for microbial consortia that self-mediate electron transfer. *Appl Environ Microb.*, **70**, 5373–5382.
- Rabaey, K., Clauwaert, P., Aelterman, P. and Verstraete, W.,** 2005b. Tubular microbial fuel cells for efficient electricity generation. *Environ Sci Technol.*, **39**, 8077–8082.
- Rabaey, K., Van De Sompel, K., Maignien, L., Boon, N., Aelterman, P. and Clauwaert, P.,** 2006. Microbial fuel cells for sulfide removal. *Environ Sci Technol.*, **40**, 5218–5224.
- Rhoads, A., Beyenal, H. and Lewandowski, Z.,** 2005. Microbial fuel cell using anaerobic respiration as an anodic reaction and biomineralized manganese as a cathodic reactant. *Environ Sci Technol.*, **39**, 4666–4671.
- Ringeisen, BR., Henderson, E., Wu, PK., Pietron, J., Ray, R. and Little, B.,** 2006. High power density from a miniature microbial fuel cell using *Shewanella oneidensis* DSP10. *Environ Sci Technol.*, **40**, 2629–2634.
- Rosenbaum, Schroder, U. and Scholz, F.,** 2006. Investigation of the electrocatalytic oxidation of formate and ethanol at platinum black under microbial fuel cell conditions. *J Solid State Electrochem.*, **10**, 872–878.
- Rozendal, RA., Hamelers, HVM. and Buisman, CJN.,** 2006. Effects of membrane cation transport on pH and microbial fuel cell performance. *Environ Sci Technol.*, **40**, 5206–5211.
- Scholz, F. and Schroder, U.,** 2003. Bacterial batteries. *Nat Biotechnol.*, **21**, 1151–1152.
- Schroder, U., Nieben, J. and Scholz, F.,** 2003. A generation of microbial fuel cells with current outputs boosted by more than one order of magnitude. *Angew Chem Int Ed.*, **42**, 2880–2883.
- Shantaram, A., Beyenal, H., Veluchamy, RRA. and Lewandowski, Z.,** 2005. Wireless sensors powered by microbial fuel cells. *Environ Sci Technol.*, **39**, 5037–5042.

- Stirling, J.L., Bennetto, H.P., Delaney, G.M., Mason, J.R., Roller, S.D. and Tanaka, K.,** 1983. Microbial fuel cells. *Biochem Soc Trans.*, **11**, 451–453.
- Straub, K.L., Benz, M. and Schink, B.,** 2001. Iron metabolism in anoxic environments at near neutral pH. *FEMS Microbiol Ecol.*, **34**, 181–186.
- Suzuki, S., Karube, I. and Matsunaga, T.,** 1978. Application of a biochemical fuel cell to wastewater. *Biotechnol Bioeng Symp.*, **8**, 501–511.
- Tartakovsky, B. and Guiot, S.R.,** 2006. A comparison of air and hydrogen peroxide oxygenated microbial fuel cell reactors. *Biotechnol Prog.*, **22**, 241–246.
- Tender, L.M., Reimers, C.E., Stecher, H.A., Holmes, D.E., Bond, D.R. and Lowy, D.A.,** 2002. Harnessing microbially generated power on the seafloor. *Nat Biotechnol.*, **20**, 821–825.
- Tokuji, I. and Kenji, K.,** 2003. Vioelectrocatalyses-based application of quinoproteins and quinprotein-containing bacterial cells in biosensors and biofuel cells. *Biochim Biophys Acta.*, **1647**,121–126.
- Vega, C.A. and Fernandez, I.,** 1987. Mediating effect of ferric chelate compounds in microbial fuel cells with *Lactobacillus plantarum*, *Streptococcus lactis*, and *Erwinia dissolvens*. *Bioelectrochem Bioenerg.*, **17**, 217–222.
- Wilkinson, S.,** 2000. “Gastrobots” — benefits and challenges of microbial fuel cells in food powered robot applications. *Auton Robot.*, **9**, 99–111.
- Zhao, F., Harnisch, F., Schroder, U., Scholz, F., Bogdanoff, P. and Herrmann, I.,** 2005. Application of pyrolysed iron(II) phthalocyanine and CoTMPP based oxygen reduction catalysts as cathode materials in microbial fuel cells. *Electrochem Commun.*, **7**, 1405–1410.
- Zhao, F., Harnisch, F., Schroder, U., Scholz, F., Bogdanoff, P. and Herrmann, I.,** 2006. Challenges and constraints of using oxygen cathodes in microbial fuel cells. *Environ Sci Technol.*, 5193–5299.
- Zuo, Y., Maness, P.C., and Logan, B.E.,** 2006. Electricity production from steamexploded corn stover biomass. *Energ Fuel.*, **20**, 1716–1721.

CURRICULUM VITAE

Candidate's full name: Berfin Hatice ATAMERT

Place and date of birth: Şişli – 22.01.1986

Permanent Address: Atatürk Cad. Osmanlı Ap. No: 19 D: 11 K:3 Erenköy/İstanbul

**Universities and
Colleges attended:** Cumhuriyet University